AGU ADVANCING EARTH AND SPACE SCIENCES

AGU Advances

RESEARCH ARTICLE
10.1029/2026AV002350

Large Overestimation of Projected Western U.S. Wildfire Burned Forest Area With Warming

Yu Cheng[1,2], **Kaighin A. McColl**[2,3], **Loretta J. Mickley**[3], **and Xu Feng**[3]

[1]Shanghai Key Laboratory of Ocean-land-atmosphere Boundary Dynamics and Climate Change, Department of Atmospheric and Oceanic Sciences, Fudan University, Shanghai, China, [2]Department of Earth and Planetary Sciences, Harvard University, Cambridge, MA, USA, [3]School of Engineering and Applied Sciences, Harvard University, Cambridge, MA, USA

Peer Review The peer review history for this article is available as a PDF in the Supporting Information.

Key Points:

- Wildfires in western U.S. forests burn hotter and spread farther when fuel is drier
- Studies using vapor pressure deficit as a proxy for land dryness claim that burned area will increase dramatically with climate warming
- Using a more appropriate proxy (soil moisture), we find that burned area will increase by much less than expected

Supporting Information:

Supporting Information may be found in the online version of this article.

Correspondence to:

K. A. McColl,
kmccoll@seas.harvard.edu

Citation:

Cheng, Y., McColl, K. A., Mickley, L. J., & Feng, X. (2026). Large overestimation of projected western U.S. wildfire burned forest area with warming. *AGU Advances*, *7*, e2026AV002350. https://doi.org/10.1029/2026AV002350

Received 7 FEB 2026
Accepted 3 APR 2026

Author Contributions:

Conceptualization: Kaighin A. McColl
Data curation: Yu Cheng, Loretta J. Mickley, Xu Feng
Formal analysis: Yu Cheng, Kaighin A. McColl
Funding acquisition: Kaighin A. McColl
Investigation: Yu Cheng
Methodology: Yu Cheng, Kaighin A. McColl
Supervision: Kaighin A. McColl
Visualization: Yu Cheng
Writing – original draft: Yu Cheng, Kaighin A. McColl

Abstract Wildfires are projected to increase with warming in the western United States. Since vapor pressure deficit (VPD) is highly correlated with wildfire burned area historically, many studies have argued that large projected increases in VPD with warming imply large increases in burned area. Here, we argue that those projections are overestimated by as much as an order-of-magnitude. First, we show that both soil moisture and VPD are well correlated with historical burned forest area. Second, we demonstrate that projected changes in VPD with warming are much larger than those in soil moisture, leading to wildly divergent projections of burned forest area: with 3 K (4 K) of warming relative to pre-industrial, the VPD-based projection is about 16 (66) times the historical burned area, whereas the soil moisture-based projection is only 2 (3) times the historical burned area. A similar divergence arises in more complex models that include VPD as only one of many explanatory variables. Third, we argue that the VPD-based projections are incorrect. VPD is used as a measure of atmospheric evaporative demand, but recent advances have demonstrated that VPD and related quantities are actually poor measures of atmospheric evaporative demand and overstate projected drying with warming. We conclude that the rate at which wildfire burned forest area will increase with warming has been greatly overestimated by some studies.

Plain Language Summary Wildfires burn hotter and spread farther when fuel is drier. Many studies have argued that climate change will make fuel much drier in the western U.S., but these studies used the vapor pressure deficit—a measure of atmospheric dryness—as an indirect measure of fuel dryness. Recent advances in terrestrial hydrology show that this is a poor approximation. Instead, we use soil moisture, a measure of land surface dryness that is more relevant to wildfire fuel, to show that wildfire burned forest area increases much less than expected with warming.

1. Introduction

Wildfires in the western United States have increased in size and intensity in recent decades (Abatzoglou & Williams, 2016; Dennison et al., 2014; Holden et al., 2018; Juang et al., 2022; Westerling, 2016; Williams et al., 2019), resulting in significant impacts on human health through smoke exposure (Aguilera et al., 2021; Connolly et al., 2024; Liu et al., 2017) and billions of dollars in economic damage (Bayham et al., 2022). How will wildfires change as the planet warms? Climate models do not typically simulate wildfires, so projections are often attained by statistically relating one or more simulated variables with wildfire burned area over the historical record, and then combining the statistical relation with projections of the simulated variables (Abatzoglou et al., 2021; Brey et al., 2021; Flannigan et al., 2005; Littell et al., 2018; Price & Rind, 1994; Spracklen et al., 2009; Turco et al., 2023; Westerling, Bryant, et al., 2011; Westerling, Turner, et al., 2011; Yue et al., 2013). In the western United States, choices for simulated explanatory variables include combinations of air temperature (Littell et al., 2009), precipitation (Holden et al., 2018), drought indices (Brown et al., 2021; Littell et al., 2009), potential evaporation (Abatzoglou & Kolden, 2013), and the difference between potential and actual evaporation (Littell & Gwozdz, 2011), among others.

A growing literature uses the vapor pressure deficit (VPD, the difference between the saturation vapor pressure and the actual vapor pressure) as a key explanatory variable in understanding wildfire burned area in the western United States (Clarke et al., 2022; Dahl et al., 2023; He et al., 2025; Higuera & Abatzoglou, 2021; Juang et al., 2022; Mueller et al., 2020; Parks & Abatzoglou, 2020; Seager et al., 2015; Williams et al., 2013, 2014, 2019; Zhuang et al., 2021). VPD is highly correlated with historical wildfire burned area in the western United

Writing – review & editing: Yu Cheng, Kaighin A. McColl, Loretta J. Mickley, Xu Feng

States (Abolafia-Rosenzweig et al., 2022; Mueller et al., 2020; Williams et al., 2014, 2019). The proposed reason for this strong correlation is that VPD is a measure of atmospheric evaporative demand, with higher VPD causing drier vegetation that burns more readily (Anderson, 1936; Pechony & Shindell, 2009; Ray et al., 2005; Seager et al., 2015; Sedano & Randerson, 2014; Silvestrini et al., 2011). Since VPD rises rapidly with warming, projections that rely at least in part on VPD (which we refer to as "VPD-based projections") typically project large increases in wildfire burned area given sufficient warming (Abatzoglou et al., 2021; Brey et al., 2021).

However, it is not obvious why VPD, a measure of *atmospheric dryness*, is a more appropriate proxy for fuel dryness than alternatives, particularly climate model-simulated measures of *land surface dryness*, such as soil moisture. While soil moisture differs from fuel moisture in various respects, most climate models do not directly simulate fuel moisture, and soil moisture seems a closer analog to fuel moisture than VPD. Since dead fuel sits on the land surface, its moisture content is determined by a water balance that is similar to the water balance determining soil moisture. Indeed, prior work has shown that soil moisture and fuel moisture are well correlated (Lu & Wei, 2021; Pellizzaro et al., 2007; Qi et al., 2012; Sharma et al., 2020), and that soil moisture, in turn, is well correlated with wildfire burned area in the western United States (Brey et al., 2021). Thonicke et al. (2001) directly simulate fuel moisture as soil moisture in the Lund-Potsdam-Jena (LPJ) Dynamic Global Vegetation Model. As a result, soil moisture is a strong predictor of various aspects of wildfires, including fire size (Holden et al., 2025; Krueger et al., 2023).

As it turns out, projections of wildfire burned area are particularly sensitive to the choice to include VPD. Brey et al. (2021) constructed a multivariate statistical model for burned area in several parts of the western U.S. that included wind speed, precipitation, soil moisture, relative humidity (RH) and VPD as explanatory variables. While eliminating VPD as an explanatory variable did not substantially reduce the model's correlation with historical burned area, it reduced the projected end-of-century burned area. In one region (the Rocky Mountains), it reduced the projected burned area by about an order-of-magnitude.

However, the implications of this sensitivity remain unclear: are the more severe VPD-based projections correct or not? In this study, we argue that they are not. First, we show that, in the western United States, historical burned forest area (Figure 1a) is highly correlated with both VPD (Figure 1b) and soil moisture (Figure 1c). Second, using outputs from the Coupled Model Intercomparison Project Phase 6 (CMIP6) (Eyring et al., 2016; Juckes et al., 2020; Copernicus Climate Change Service (C3S), 2021) spanning 12 climate models and four socioeconomic pathways (Table S1 in Supporting Information S1), we show that VPD-based projections of burned area are as much as an order-of-magnitude larger than soil moisture-based projections, consistent with Brey et al. (2021). These projections are derived from observed linear relations between the logarithm of historical burned area and either VPD or soil moisture. We also obtain qualitatively similar results using more complex multivariate statistical models incorporating other variables. Third, we examine this divergence by reviewing recent advances in our understanding of atmospheric evaporative demand and its changes in a warming world, all of which suggest the VPD-based projections are large overestimates. In particular, we argue that projections that include VPD as an explanatory variable (including those based on many common wildfire indices) should be expected to severely overestimate future burned area, given sufficient warming.

2. Methods

2.1. Study Region

We focused on forested regions in the continental United States west of 100°W (Figure 1a), where fire activity is generally limited by flammability rather than fuel availability (Abatzoglou et al., 2018; Krawchuk & Moritz, 2011). Focusing on forested regions is also consistent with the most relevant prior studies (Abatzoglou & Williams, 2016; Holden et al., 2018; Juang et al., 2022; Parks & Abatzoglou, 2020). Fractional forest cover at 1-km resolution is obtained from Juang et al. (2022), derived from 250-m forest type maps based on the U.S. Forest Service Forest Inventory and Analysis (FIA) program (Ruefenacht et al., 2008).

In addition to analyzing burned area averaged across all forests in the entire western United States, we also examined subregions defined by ecoregions. The five aggregated ecoregions (Figure S1 in Supporting Information S1) were derived from the EPA Level II Ecoregion data set (U.S. Environmental Protection Agency, 2024). The five ecoregions are (a) Northwestern Forested Mountains, (b) Mediterranean California, (c) Cold Deserts, (d) Southwestern Forested Mountains, and (e) Central Prairies. Forest cover is proportionally

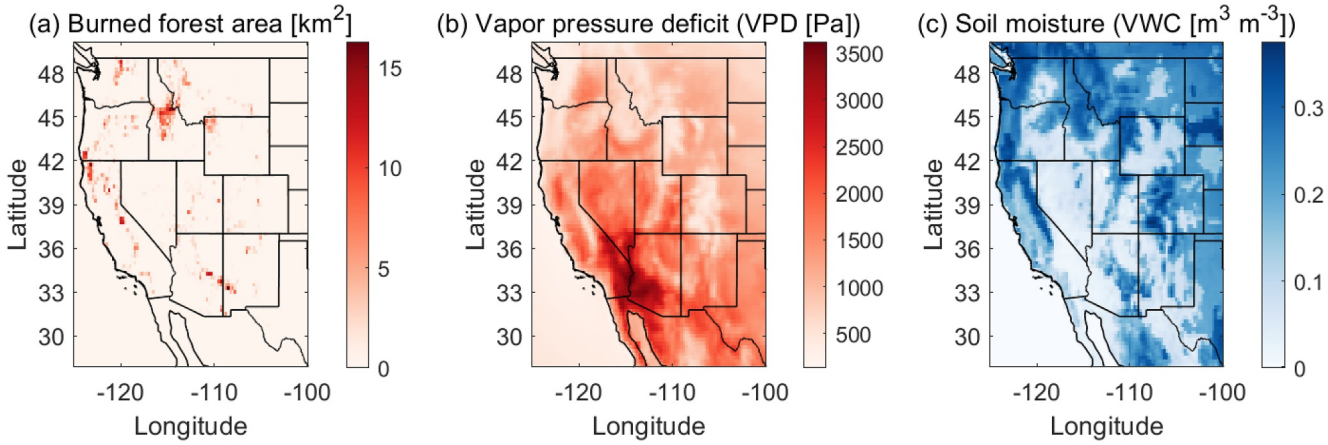

Figure 1. (a) Total burned forest area averaged over the 6-month fire season (May–October) for 1984–2014 from the Western U.S. MTBS-Interagency wildfire database (Juang et al., 2022). (b) Vapor pressure deficit from ERA5 for the same period. (c) Volumetric water content in the soil from ERA5 for the same period.

greater in ecoregions 1 and 4 than in ecoregions 2, 3, and 5 (Feng et al., 2025). Over the period 1984–2014, burned forest area in ecoregions 1–5 accounted for 73.2%, 4.6%, 7.9%, 12.7%, and 1.9% of the total burned forest area in the western United States, respectively (Table S2 in Supporting Information S1).

2.2. Wildfire Database

We used the Western U.S. MTBS-Interagency (WUMI) wildfire data set developed by Juang et al. (2022), which includes 18,368 wildfire events over 1 km^2 across the western United States from 1984 to 2020. The WUMI data set (Juang & Williams, 2024) includes the following wildfires: large wildfires (≥1,000 acres ≈ 4 km^2) from the Monitoring Trends in Burn Severity program (Eidenshink et al., 2007) and wildfires ≥1 km^2 from the National Wildfire Coordinating Group and the California Department of Forestry and Fire Protection. The forest area burned for each fire was estimated by multiplying the total burned area by the corresponding fractional forest cover. The analyzed fire events were restricted to fires that ignited during the 6-month fire season (May–October), when fires in the western U.S. generally occur (Juang et al., 2022; Spracklen et al., 2009). The logarithm of the total burned forest area from May to October serves as the predictand in the linear model.

2.3. Reanalyses

To statistically relate burned area to soil moisture and VPD, we used outputs from three different reanalyses. First, we used outputs from the fifth generation ECMWF reanalysis (ERA5; Copernicus Climate Change Service (C3S), 2023; Hersbach et al., 2020, 2023). ERA5 is a global atmospheric reanalysis in which the land surface evolves within a coupled forecast model and is further constrained by a land data assimilation system that adjusts soil moisture and other surface variables using screen-level and satellite observations. The horizontal spatial scale of the reanalysis is approximately 31 km (Hersbach et al., 2020). Monthly mean 2-m air temperature and dewpoint temperature were used to compute monthly mean saturation vapor pressure (e_s, estimated using the Magnus approximation (Alduchov & Eskridge, 1996)) and actual vapor pressure (e_a), which were further used to compute VPD (Figure 1b). We also used topsoil volumetric soil water content (VWC) averaged over the upper 0–7 cm of soil (swvl1, Figure 1c). Volumetric soil water content in ERA5 is simulated within the Integrated Forecast System using the Carbon Hydrology-Tiled ECMWF Scheme for Surface Exchanges over Land land surface model (CHTESSEL; Balsamo et al., 2009).

Second, we used outputs from the ERA5-Land reanalysis (Muñoz-Sabater et al., 2021). This product is derived by running the CHTESSEL land surface model offline (the same model used within ERA5, but here decoupled from the atmosphere) and forced by downscaled ERA5 near-surface meteorology, downwelling radiation, and precipitation. The model is run at a higher spatial resolution (~9 km) than ERA5 (~31 km). While observations are assimilated in ERA5, they are not directly assimilated in ERA5-Land. Observations only influence the land surface in ERA5-Land indirectly, through the ERA5 atmospheric forcings. As for ERA5, we used monthly mean

2-m air temperature (t2m) and dewpoint temperature (d2m) to compute VPD, and topsoil volumetric soil water content averaged over the upper 0–7 cm of soil (swvl1).

Third, we used outputs from the Modern-Era Retrospective analysis for Research and Applications, version 2 (MERRA-2) reanalysis (Gelaro et al., 2017). Like ERA5, MERRA-2 is a global atmospheric reanalyis in which the land surface evolves within a coupled forecast model. The horizontal spatial scale is ∼50 km, and thus coarser than ERA5 or ERA5-Land. Unlike ERA5, it does not include a land data assimilation system that adjusts soil moisture (and other surface variables) using screen-level observations. Instead, the land surface is forced with observation-corrected precipitation (Reichle et al., 2017), rather than model-generated precipitation, as in ERA5 and ERA5-Land. We used monthly mean 2-m air temperature (T2M) and dewpoint temperature (T2MDEW) to compute VPD, and topsoil volumetric soil water content averaged over the upper 0–5 cm of soil (SFMC). Volumetric soil water content in MERRA-2 is simulated using the Catchment land surface model (Koster et al., 2000).

For all three reanalyses, data averaged over the 6-month fire season (May–October) for each year during 1984–2014 were used as historical observations for model calibration. We were restricted to this time period because the CMIP6 historical period ends in 2014 (discussed further below), although results are qualitatively similar if the time period is extended closer to the present (not shown). Forest-area-weighted averages over the study region were used, as in Juang et al. (2022).

Why not use satellite and/or station observations of VPD and soil moisture instead of reanalyses? High-quality collocated observations of soil moisture and VPD spanning this period do not exist. In addition, observations of soil moisture are subject to much larger errors than observations of VPD, which can lead to the appearance that VPD is the more important control on burned area, even when it is not. We discuss this issue in more detail in Section 3.1. While reanalysis soil moisture is also likely subject to greater errors than reanalysis VPD, the problem is partially mitigated by the reanalysis attempting to reconcile observations with a model that couples soil moisture and VPD. Soil moisture has been ground-truthed, to varying extents, in ERA5 (Dorigo et al., 2021; Muñoz-Sabater et al., 2021), MERRA-2 (Reichle et al., 2017) and ERA5-Land (Muñoz-Sabater et al., 2021).

2.4. Climate Model Projections

To project burned forest area, we used climate model projections from CMIP6 experiments (Copernicus Climate Change Service (C3S), 2021; Eyring et al., 2016; Juckes et al., 2020). Monthly mean 2-m air temperature was used to compute monthly mean saturation vapor pressure, which was then combined with near-surface specific humidity to compute RH and VPD. The mass of water in the top 10-cm surface soil layer was used to compute volumetric water content (VWC). We used CMIP6 outputs from the SSP1-2.6, SSP2-4.5, SSP3-7.0, and SSP5-8.5 experiments and from 12 climate models averaged over the six-month fire season (May–October) for each year (Table S1 in Supporting Information S1). The 12 models (listed in Table S1 in Supporting Information S1) were selected because they provided the complete set of variables required for our projections. These scenarios span a broad range of future socioeconomic pathways and radiative forcing trajectories, from strong mitigation (SSP1–2.6) to high-emissions futures (SSP5–8.5) (O'Neill et al., 2016). Projections spanned the period 2015–2099. To eliminate dependence on a specific climate projection, the global mean warming, defined as the difference between global mean temperature for each year and the global mean temperature over 1850–1900 (NOAA National Centers for Environmental Information, 2025), was used to characterize the strength of warming instead of calendar year (Matthews et al., 2017).

2.5. Statistical Projections of Burned Area

To estimate future changes in burned forest area, we developed empirical relations between historical burned area and anomalies of VPD and VWC. More specifically, we performed linear regressions between the logarithm of total burned forest area in the western United States and reanalysis VPD (or VWC) anomalies, calculated relative to the long-term VPD (or VWC) average over the period 1984–2014. Prior studies have shown that the logarithm of burned forest area is well correlated with VPD in the western United States (Abatzoglou & Williams, 2016; Abatzoglou et al., 2018; Juang et al., 2022; Williams et al., 2019). Following Juang et al. (2022), the forest-area-weighted average of the VPD or VWC anomaly was used. The linear regression model was fit to the period 1984–2014 to align with the CMIP6 historical period, which ends in 2014. These linear regressions were then applied to VPD and VWC projections from CMIP6 data sets to estimate future burned forest area. For each

regression, we estimated 95% confidence intervals on the estimated Pearson correlation coefficients using bootstrapping with 10,000 replicates. We did this because it is common in prior wildfire studies to use the correlation coefficient as a measure of model performance. However, this approach does not penalize overfitting, which can cause high within-sample correlation but poor out-of-sample prediction. To address this issue, we also estimated the Akaike Information Criterion (AIC; Akaike, 1998) for each model, with a bias-correction for small sample size (Hurvich & Tsai, 1989)

$$\mathrm{AIC}_c = \underbrace{-2\log\left(\mathcal{L}\left(\hat{\theta}\right)\right) + 2k}_{\mathrm{AIC}} + \frac{2k(k+1)}{n-k-1}, \tag{1}$$

where n is the sample size, k is the number of parameters (in an ordinary least squares regression with one independent variable, $k = 3$, which includes the slope, offset and error variance) and $\mathcal{L}\left(\hat{\theta}\right)$ is the likelihood function given estimated parameters $\hat{\theta}$. The AIC_c was estimated for each statistical model. The AIC_c accounts for overfitting by penalizing models with more parameters. While the absolute values are meaningless, relatively lower values indicate a relatively better model. However, this ranking is impacted by sampling uncertainty, which is not accounted for by the Hurvich and Tsai (1989) bias-correction, and is especially relevant here due to the relatively low sample size in our analysis. To account for sampling uncertainty in model selection, we used bootstrapping with 10,000 replicates to repeat the process by sampling with replacement from the observations, and report the fraction of replicates in which each model was selected as the best model (Burnham et al., 2010, Section 4.5.2).

We used soil moisture anomalies rather than absolute soil moisture in our regression because absolute soil moisture levels vary substantially between CMIP6 models, whereas anomalies exhibit greater consistency and comparability across models (Koster et al., 2009). For soil moisture from each CMIP6 model under each emission scenario, the anomaly was defined as the difference between the western U.S. fire-season average in a given year and the long-term regional fire-season mean over the historical period (1984–2014). For consistency, we used VPD anomalies instead of absolute values of VPD. In presenting results in Figure 3, future projections of VPD anomaly, soil moisture anomaly, and burned forest area were averaged within global mean warming bins of 0.5 K for all emission scenarios, to smooth out interannual variability.

We also tested our approach using more complex models. To that end, we constructed burned forest area projections using multivariate regressions calibrated over the same historical period. The regressions included combinations of the following explanatory variables derived from the ERA5 reanalysis: air temperature, precipitation, RH, wind speed, VPD, runoff, and soil moisture. This set of seven variables matched those used in Qiu et al. (2025), which focused on smoke exposure from wildfires, and is consistent with the variables used in prior multivariate approaches. For consistency with our univariate regressions, we used anomalies rather than absolute values for each variable. We then conducted four sets of multivariate regressions to isolate the effect of VPD and air temperature. First, we included all seven variables as predictors. Second, we excluded temperature and used the remaining six variables. Third, we excluded VPD and used the remaining six variables. Fourth, we excluded both temperature and VPD and used the remaining five variables.

3. Results and Discussion

3.1. Soil Moisture and VPD Are Both Correlated With Historical Burned Area

VPD anomalies were strongly positively correlated with log-transformed burned forest area, for all three reanalyses (Figures 2a, 2c, and 2e). The reported R^2 value is the squared Pearson correlation coefficient and corresponds to the fraction of variance explained by the linear regression. VPD from ERA5 and ERA5-Land both explained approximately 75% of the variance in burned forest area; VPD from MERRA-2 explained a little less (approximately 60%). This is consistent with previous studies (Abatzoglou & Williams, 2016; Parks & Abatzoglou, 2020), which found that VPD-burned area R^2 values were as strong as, or stronger than, other climate variables, including temperature, precipitation, and various aridity indices. The R^2 value between log-transformed burned forest area and VPD anomalies varied between ecoregions (Tables S2–S4 in Supporting Information S1). For all three reanalyses, in ecoregions 1 and 4, the R^2 values were comparable to those for the entire western U.S., whereas R^2 values in ecoregions 2, 3, and 5 were notably lower. This pattern was consistent with the higher proportion of forest cover in ecoregions 1 and 4 relative to ecoregions 2, 3, and 5. Somewhat similar variability in

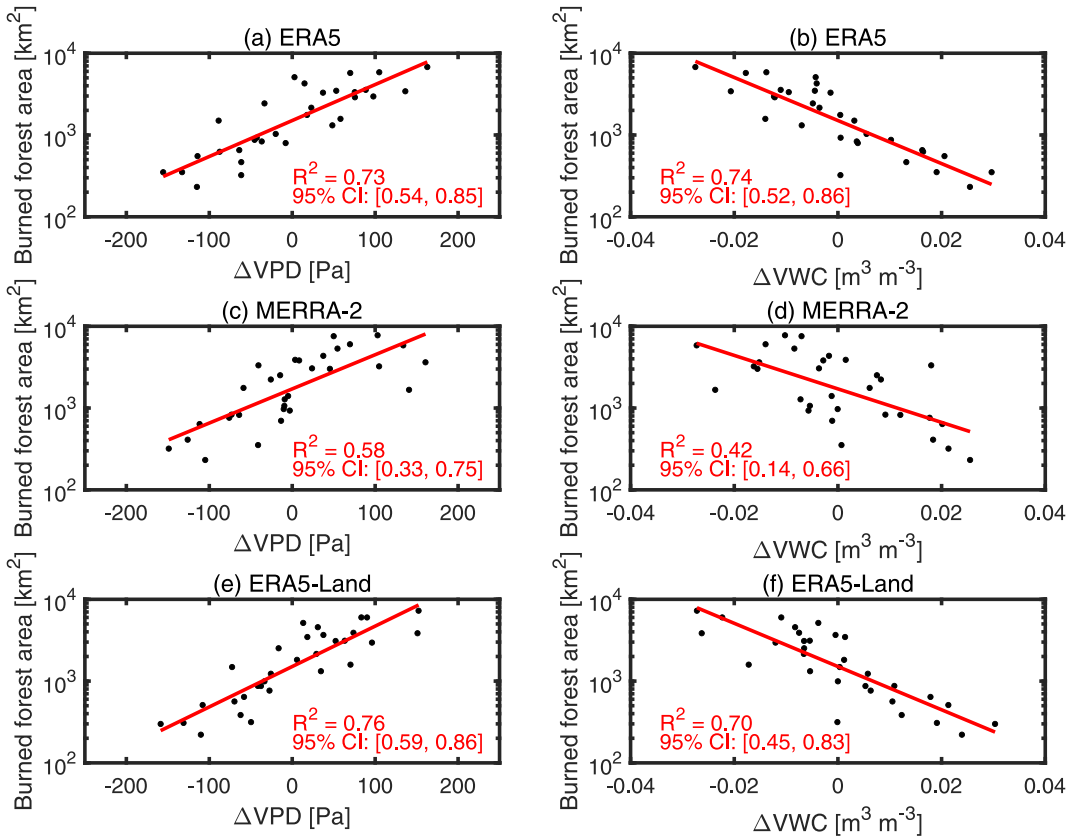

Figure 2. Both soil moisture and vapor pressure deficit (VPD) are well correlated with burned area in forested regions of the western U.S. over the historical record, even though soil moisture observations are much less accurate than VPD observations. (a) Scatter plot of annual burned forest area in the 6-month fire season (May–October) versus the VPD anomaly computed from ERA5 over the period 1984–2014. The forest-area-weighted average VPD is used to represent VPD over the study region. The VPD anomaly (ΔVPD) is defined as the difference between the fire-season average in each year and the long-term (1984–2014) fire-season mean over the same period. The R^2 value and the 95% confidence intervals for the R^2 estimate are also shown. Panel (b) same as (a) but using soil moisture (volumetric water content) instead of VPD. Panels (c, d) same as (a, b) but using MERRA-2 reanalysis data. Panels (e, f) same as (a, b) but using ERA5-Land reanalysis data.

R^2 values across ecoregions was reported in a previous study (Yue et al., 2013), although different regression input variables were used. The lower R^2 values in ecoregion 2 may be due to the region's relatively dense population resulting in a greater proportion of human-caused fires (Feng et al., 2025).

Soil moisture anomalies were also strongly (negatively) correlated with log-transformed burned forest area, for all three reanalyses (Figures 2b, 2d, and 2f). Soil moisture anomalies explained similar fractions of the variance in burned forest area, with MERRA-2 again explaining a little less than ERA5 and ERA5-Land. The R^2 values between soil moisture anomalies and burned area varied among ecoregions, but in a manner similar to those between VPD and burned area (Tables S2–S4).

An important distinction between soil moisture and VPD was not accounted for in these statistical comparisons: observations of soil moisture are subject to much larger errors than observations of VPD. First, VPD is mainly measured in situ at weather stations, whereas soil moisture is mainly observed remotely by satellites from space, and this is reflected in the reanalyses. Microwave satellite observations of soil moisture are least accurate in forests (Entekhabi et al., 2010; Jackson & Schmugge, 1991), which makes them less informative in studying forest fires. To the extent that point-scale soil moisture measurements are available, they are far less common than point-scale measurements of VPD. Second, even if point-scale in situ measurements of soil moisture were as common as those for VPD, they contain large "representativeness errors" that dwarf those for VPD. The representativeness error is the difference between a point-scale measurement of a quantity (or an average of several point-scale measurements) and the larger-scale average of the quantity (Gruber et al., 2016). VPD exhibits

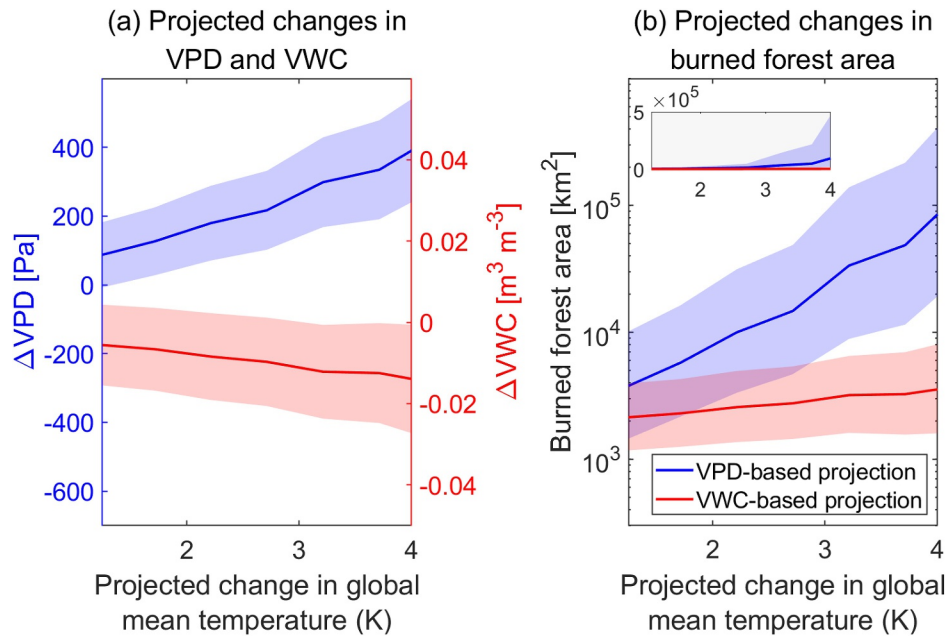

Figure 3. Vapor pressure deficit (VPD)-based projections of burned area are much larger than soil moisture-based projections. (a) VPD anomaly (ΔVPD) and soil moisture anomaly (ΔVWC) from CMIP6 projections over 2015–2099 plotted against the global mean warming since pre-industrial (1850–1900). For each socioeconomic pathway (SSP1-2.6, SSP2-4.5, SSP3-7.0, and SSP5-8.5), we calculate the multi-model mean change in VPD and volumetric water content (VWC) and their inter-model standard deviations across the CMIP6 ensemble. We then combine the results from all pathways and compute bin-averaged values within 0.5 K intervals of global-mean temperature change. The shaded region indicates the multi-model mean ± one standard deviation. (b) VPD-based and VWC-based projections of burned forest area. The inset in the upper left reproduces the main panel but with a linear *y*-axis in place of the logarithmic scale.

much less spatial variability than soil moisture, because it is a property of the well-mixed, fluid atmosphere, whereas soil moisture is a property of the heterogeneous, solid land surface (Vargas Zeppetello et al., 2023) and varies significantly on spatial scales as small as a few centimeters (Famiglietti et al., 2008; Feldman et al., 2023; Western et al., 2002). Thus, even if soil moisture and VPD actually both contributed equally to causing wildfires, we would expect that observed soil moisture should correlate less well with burned area than observed VPD, simply because the soil moisture observations are less accurate. This could even be true if VPD does not impact wildfires at all, so long as large-scale variability in soil moisture causes large-scale variability in both VPD and burned area (discussed further in Section 3.3).

For these reasons, it would be unjustified to claim that VPD is more important than soil moisture in understanding and projecting burned area based solely on a stronger R^2 value with burned area, or a lower AIC_c. With this caveat in mind, for completeness, model selection rates based on the AIC_c are shown in Tables S5–S7 in Supporting Information S1. The soil moisture-based burned area model was selected as better in 56% of bootstrap replicates in ERA5, 1% of replicates in MERRA-2, and in 17% of replicates in ERA5-Land. The model selection rates further varied between ecoregions. Given that major differences in observation errors between soil moisture and VPD were not accounted for in these statistics, it is not possible to conclude that one model is better than the other solely from these statistical analyses. It is clear, however, that both soil moisture and VPD correlate well with burned area over the historical record. Since this basic finding is robustly reproduced in all three reanalyses, we focus solely on the ERA5 reanalysis for the remainder of the study, unless stated otherwise.

Adding more explanatory variables did not improve on the univariate soil moisture or VPD models when overfitting was appropriately penalized. When comparing both univariate and multivariate models, no model was consistently selected as best across bootstrap replicates, based on the AIC_c (Table S8 in Supporting Information S1). The most complicated multivariate model was only selected as best in 3.5% of replicates, indicating that the additional complexity was not warranted. Qualitatively similar results were found if air temperature was excluded, VPD was excluded, or if both were excluded. In fact, out of all univariate and multivariate models, the

univariate soil moisture model was most frequently selected as best (49% of bootstrap replicates) based on the AIC_c (Table S8 in Supporting Information S1). We did not consider alternative multivariate models that select a subset of explanatory variables, such as the least absolute shrinkage and selection operator (LASSO; Tibshirani, 1996), sometimes used in prior studies (e.g., Brey et al., 2021; Qiu et al., 2025). If soil moisture observations are subject to sufficiently greater measurement errors than VPD and other variables, and soil moisture causes variability in both VPD and burned area, then the LASSO may incorrectly select VPD over soil moisture (Sørensen et al., 2015).

Overall, these results imply that there is at least as much reason, based on historical correlations, to construct statistical projections of future burned area using soil moisture as the explanatory variable, as there is using VPD as the explanatory variable. These univariate models are at least as justified as more complicated multivariate models when overfitting is penalized, as it should be.

3.2. VPD-Based Projections of Burned Area Are Much Larger Than Soil Moisture-Based Projections

Since VPD rises rapidly with warming (Figure 3a), VPD-based projections of burned area also rise rapidly with warming (Figure 3b). For example, if global temperatures rise by 3 K—which seems likely by the end of the century (IPCC, 2023)—burned area is projected to increase by a factor of about 16 (Figure S2 in Supporting Information S1 shows projections as a fraction of historical burned area). If global temperatures rise by 4 K—which is also possible by the end of the century (IPCC, 2023)– burned area is projected to increase by a factor of about 66 (Figure S2 in Supporting Information S1). This would be a truly massive increase. For example, of California's 33 million acres of forest, roughly 300,000–400,000 acres burned annually, on average, over the historical period we consider (Williams et al., 2019). A 66-fold increase in burned area would imply that wildfires would become mainly fuel-limited, with forests immediately burning once sufficient vegetation has regrown. Forests would effectively cease to exist in California in anything like their current form. For these projections, we relied on observed linear relations between historical log-transformed burned area and VPD. We also constructed burned area projections using air temperature as the explanatory variable, and found qualitatively similar results to those obtained using VPD (Figure S8 in Supporting Information S1). Prior studies have noted that VPD-based burned area projections are similar to those obtained using temperature (Turco et al., 2023). Equivalent figures are provided in Supporting Information S1 replacing global mean warming on the horizontal axis with local mean warming (Figure S3 in Supporting Information S1), local maximum temperature warming (Figure S4 in Supporting Information S1), and calendar year (Figure S5 in Supporting Information S1), which all provide qualitatively similar results.

In contrast, since changes in soil moisture are more muted (Figure 3a), soil moisture-based projections imply a much smaller increase in burned area with warming (Figure 3b). For 3 K of global mean warming, they project an increase in burned area by a factor of about two; for 4 K, an increase by a factor of about three (Figure S2 in Supporting Information S1). Qualitatively similar results were found in individual ecoregions (Figres S10–S14 in Supporting Information S1), and when redoing the analysis using MERRA-2 (Figure S15 in Supporting Information S1) and ERA5-Land (Figure S16 in Supporting Information S1). We also constructed burned area projections using RH as the explanatory variable, and found qualitatively similar results to those obtained using soil moisture (Figure S7 in Supporting Information S1). At sufficiently large spatial scales, RH is a surprisingly good proxy for soil moisture, with dry soils causing a low evaporative fraction, which, in turn, cause low RH (Betts, 2000; McColl & Rigden, 2020; McColl & Tang, 2024).

Projections remain sensitive to the inclusion of VPD and, to a lesser extent, temperature when constructed from multivariate statistical models that consider multiple predictors simultaneously (Figure S6 in Supporting Information S1). We considered four multivariate projections, based on the four statistical models described in Section 2.5. Recall that, perhaps surprisingly, none of the four multivariate models exhibited better performance than the univariate soil moisture and VPD models shown in Figure 2 (Table S8 in Supporting Information S1). This is because the AIC penalizes overfitting, and the multivariate models add parameters without substantially improving the model's fit to the data. The multivariate projection including all seven variables (including VPD and air temperature) produced the largest projected burned forest area (Figure S6 in Supporting Information S1)—9.2 (32) times the historical burned area with 3 K (4 K) of warming. Very similar projections were obtained when temperature was excluded and only the remaining six variables were used. In contrast, removing VPD as a predictor resulted in large reductions in projected burned area. Simply removing VPD from the

multivariate projection and retaining the other six variables reduced projected burned area to 4.9 (9.9) times the historical burned area with 3 K (4 K) of warming. Excluding both temperature and VPD and retaining the remaining five variables reduced the projected burned area to just 2.0 (3.0) times the historical burned area with 3 K (4 K) of warming. Notably, projections excluding both temperature and VPD yielded burned area estimates comparable to those obtained using soil moisture alone (Figure 3b).

In short, statistical model projections are systematically much larger when VPD (or, to a lesser extent, air temperature) is included as a predictor, consistent with Brey et al. (2021). This is true for both multivariate and univariate models. The inclusion of VPD in the multivariate model projection is the key reason behind the large divergence between different projections derived from the different multivariate models. This further justifies our referring to multivariate model projections that include VPD as "VPD-based projections" and our earlier focus on univariate VPD projections.

3.3. VPD-Based Projections Are Incorrect Based on Prior Literature

Given the large disagreement between VPD- and soil moisture-based projections of burned area, they cannot both be correct. To our knowledge, one prior study has noted the divergence between VPD- and soil moisture-based projections (Brey et al., 2021), but did not make a case for one being incorrect. Here, we argue that the VPD-based projections are incorrect, based on physical arguments published in the last decade in the field of terrestrial hydrology. In this section, we review and synthesize that literature, which does not appear to be widely known in the wildfire community.

Why use VPD to predict burned area? Seager et al. (2015) offer a concise mechanistic explanation, based on the arguments of Anderson (1936): "It is not surprising that VPD is more successful in explaining burned forest fire area than are other meteorological variables. It is essentially a measure of the ability of the atmosphere to extract moisture from the surface vegetation, thus reflecting variations in the moisture content and flammability of forests." What Seager et al. (2015) call "a measure of the ability of the atmosphere to extract moisture from the surface" is often referred to as "atmospheric evaporative demand" or "potential evapotranspiration" (PET) in hydrology, equivalent to the evapotranspiration (ET) that would arise at a time or place if there was abundant water to evaporate. More precisely, PET is often estimated using the Penman equation, which relates PET to VPD:

$$\lambda \mathrm{PET} = \frac{\epsilon R_n + \rho \lambda g_a \overbrace{q^*(T_a)(1-\mathrm{RH})}^{\mathrm{VPD}}}{\epsilon + 1} \tag{2}$$

where λ is the latent heat of vapourization of water, R_n is surface net shortwave and longwave radiation, $\epsilon = \frac{\lambda}{c_p}\frac{\lambda q^*(T_a)}{R_v T_a^2}$, c_p is the specific heat capacity of air at constant pressure, $q^*(T_a)$ is the saturation specific humidity, a strong increasing function of air temperature (T_a), R_v is the specific gas constant of water vapor, ρ is air density, g_a is the aerodynamic conductance, and RH is relative humidity. The ground heat flux has been neglected given it is typically small on time scales longer than a day, although it can be easily included if desired. VPD is in the numerator of this equation and, since $q^*(T_a)$ and hence VPD rises rapidly with warming, the Penman equation predicts that PET will also rise rapidly with warming. This characteristic is also true of variants of the Penman equation, such as the FAO-56 reference crop equation (Allen et al., 1998) and other variants that incorporate plant physiological responses to rising carbon dioxide (Yang et al., 2019). We refer to all projections based on these measures as "VPD-based projections", even though other quantities are also used in the Penman equation and its variants.

The problem with this argument is that VPD is, empirically, a poor measure of atmospheric evaporative demand. Milly and Dunne (2016) examined times and places in climate models where ET was not water-limited, such that ET = PET. They showed that, in climate models, surface net radiation (R_n) multiplied by a constant was empirically a much better predictor of PET than other options, including the Penman equation. Maes et al. (2019) performed a similar analysis, but used eddy covariance measurements of ET under unstressed conditions rather than results from climate models. They found a similar result: PET primarily scales with surface net radiation, not VPD (or other options that included VPD, such as the Penman equation).

This result is surprising because ET from a leaf in a plant chamber does, in fact, scale with VPD. How do we explain this discrepancy? In a small-scale plant chamber experiment, VPD is an exogenous forcing. At large scales relevant to climate, however, strong land-atmosphere feedbacks make VPD endogenous: it is determined, in part, by the ET arising from the land surface (Bouchet, 1963; Brutsaert & Stricker, 1979; Gallagher & McColl, 2025; Kim et al., 2023; McColl & Rigden, 2020; McColl & Tang, 2024; Morton, 1969; Tang & McColl, 2025; Zhou & Yu, 2024). As an example, VPD in a dry western U.S. forest is very large in the summer. But, if the forest was to be hypothetically flooded with water, the VPD would decline substantially, due to both cooling and moistening of the overlying air in response to the land surface change (Gallagher & McColl, 2025). This distinction is very important because PET is, by definition, the ET that would arise from a landscape if it was hypothetically flooded with water (more precisely, if it was not water-limited), even if the landscape is actually dry. The Penman equation overestimates PET by using the observed VPD, rather than the much lower VPD that would arise if the land surface was hypothetically saturated (Berg & McColl, 2021; Kim et al., 2023; Milly & Dunne, 2016; Roderick et al., 2015; Tang & McColl, 2025; Zhou & Yu, 2024, 2025a, 2025b). Several recent studies (Kim et al., 2023; Tang & McColl, 2025; Zhou & Yu, 2024, 2025a, 2025b) have shown that, if land-atmosphere feedbacks are incorporated into the Penman equation, the resulting equation for PET largely scales with R_n, as observed empirically (Maes et al., 2019; Milly & Dunne, 2016), not VPD.

As a result, VPD-based projections of aridity are grossly overstated. If a standard scaling for PET that ignores land-atmosphere feedbacks is used (like the Penman equation), then climate models project massive, widespread drying with warming (Sherwood & Fu, 2014). If PET is instead treated as scaling with R_n, then there are no obvious signs of global mean drying in exactly the same climate models (Greve et al., 2019). As it turns out, the more modest projection (based on PET scaling with R_n) is more consistent with other lines of evidence, based on climate models and proxy records (Berg & McColl, 2021; McColl et al., 2022; Roderick et al., 2015). The divergence between these different lines of evidence has been called the "aridity paradox" (Roderick et al., 2015), but if PET is simply treated as scaling with R_n, the "aridity paradox" essentially disappears (Greve et al., 2019; Kim et al., 2023; Tang & McColl, 2025; Zhou & Yu, 2025a, 2025b).

What about the fact that VPD is highly correlated with burned area over the historical record? Put simply, correlation is not causation. The "plant chamber" interpretation is that VPD is an approximately exogenous forcing, with rising VPD causing declining fuel moisture content. But at ecosystem scales relevant to climate, the causal direction is often reversed, with dry land surfaces causing dry near-surface air. Mechanism-denial experiments dating back to the earliest climate models support this claim (Becker & Stevens, 2014; Delworth & Manabe, 1989; Krakauer et al., 2010; Laguë et al., 2023; McColl & Tang, 2024; Zhou et al., 2019). In addition, the "plant chamber" interpretation predicts that VPD (and related quantities, like the Penman equation) should accurately reflect PET, which conflicts with empirical analyses of climate models (Milly & Dunne, 2016) and observations (Maes et al., 2019). In contrast, the alternative interpretation (in which dry soils cause dry air) predicts that PET should scale with R_n (Kim et al., 2023; Tang & McColl, 2025; Zhou & Yu, 2024, 2025a, 2025b), in agreement with empirical analyses. This interpretation also implies that VPD and soil moisture should be correlated over the historical record (a period in which temperatures were approximately stable), but may diverge as the planet warms (since VPD inevitably rises with warming, even if soil moisture does not change). This is consistent with climate model projections (Figure 3), whereas the "plant chamber" interpretation (that rapidly rising VPD should cause rapidly declining soil moisture) is not.

Our soil moisture-based projections are broadly consistent with independent projections in other studies that avoid statistically relating burned area and VPD. Spracklen et al. (2009) developed multivariate statistical models for burned area in different ecoregions of the western U.S. using temperature, wind, RH, precipitation, and fire weather index, but not VPD. They projected annual burned area would increase by approximately 50% relative to 1996–2005 by the 2050s, corresponding to roughly 2 K of mean warming. Even though our projections differ in various respects (including using a slightly different historical reference period, and using multiple climate models), our soil moisture-based projections are broadly consistent with Spracklen et al. (2009), whereas our VPD-based projections are not (Figure S3b in Supporting Information S1). In addition, Bhattarai et al. (2025) used a land surface model that simulates wildfires and found that burned area in the western United States would increase by a factor of 2–3 by the end of the century, corresponding to approximately 3.5–4 K of global mean warming in the emission scenarios they considered (see their Figure 3d). Again, these projections are broadly consistent with our soil moisture-based projections, but not with our VPD-based projections.

In summary, recent advances show that VPD (and the Penman equation, and similar variants) are poor measures of PET, based on both empirical (Maes et al., 2019; Milly & Dunne, 2016) and physical considerations (Kim et al., 2023; Tang & McColl, 2025; Zhou & Yu, 2024, 2025a, 2025b). They drastically overstate the response of PET to warming, leading to the erroneous impression that warming causes severe drying. The actual PET response to warming is much more subtle, resulting in some regions experiencing drying, and others experiencing wetting (Gallagher & McColl, 2025). As a result, VPD-based projections of burned area should be expected to overestimate changes with warming, and to a greater extent as warming increases.

3.4. Limitations

There are broader limitations to projections of burned area based on historical correlations, whether or not they use VPD, soil moisture or other explanatory variables. All such projections assume the historical regression relation remains stationary despite changes in climate and forest conditions. That assumption may fail due to complex and potentially non-stationary interactions between climate, vegetation, and wildfire behavior (Hurteau et al., 2019; Littell et al., 2018; McKenzie & Littell, 2017; Westerling, Turner, et al., 2011). For example, if fires become fuel-limited rather than flammability-limited (Abatzoglou et al., 2021), they will not be reflected in the historical regression relation. In addition, an overabundance of fuel in some areas of the western U.S., a result of the twentieth century practice of widespread wildfire suppression (Marlon et al., 2012; Parks et al., 2015), may also change the regression relation in the future. Such issues represent a problem with statistical projections that also characterize projections of drought, aridity and the terrestrial water cycle, more generally (McColl et al., 2022). Mechanistic models—including landscape fire models, where fire ignition and spread are explicitly modeled (Finney, 1998; Li et al., 2020; Linn et al., 2002), or dynamic vegetation models including a fire component (Pfeiffer et al., 2013; Thonicke et al., 2010)—avoid this problem, but at the cost of much greater complexity that requires parameterizing processes that may not be well understood (Williams & Abatzoglou, 2016).

3.5. Implications

What does this mean for projections of burned area? In our view, projections explicitly based on VPD or variants of the Penman equation (often referred to in the wildfire literature as "ET_0") should be expected to severely overestimate projected burned area given sufficient warming. Some recent estimates based on other fire danger indices appear to provide more conservative projections. Such indices include the "climatic water deficit" (CWD), defined as the difference between PET and ET (Abatzoglou et al., 2021), or the Palmer Drought Severity Index (PDSI; Palmer (1965)). Yet these indices still include explicit dependence on an incorrect measure of PET. It may be possible to replace those estimates of PET with variants that scale with R_n, rather than VPD, and this may be worth exploring. As one example, Gallagher and McColl (2025) propose a simple theory for soil saturation that only requires precipitation and surface net radiation as inputs, and similar approaches might reasonably extend to fuel moisture content (note that we would not expect net radiation alone to explain much variability in burned area, since both precipitation and net radiation determine soil moisture and fuel moisture). This simple theory predicts relatively minor declines in soil moisture over the western United States (Figure S9 in Supporting Information S1), consistent with climate model projections (Figure 3c), and would presumably result in more modest burned area projections. In addition, we found that the burned area projected using RH as an explanatory variable (Figure S7 in Supporting Information S1) was comparable to that based on soil moisture. It is sometimes asserted that VPD is a better measure of land surface dryness than RH (Anderson, 1936; Seager et al., 2015), but this is only true if one adopts the "plant chamber" interpretation, in which land-atmosphere feedbacks are minor. In fact, land-atmosphere feedbacks are large and imply the reverse is true. Dry soils cause a low evaporative fraction, which causes low RH, resulting in a strong causal relation between soil moisture and RH (Betts, 2000; McColl & Rigden, 2020; McColl & Tang, 2024).

What about other meteorological fire indices that do not include explicit dependence on VPD or variants of the Penman equation? Such indices include the Keetch-Byram Drought Index (KBDI; Keetch & Byram (1968)), the Fire Weather Index (FWI; Wagner, 1987), the Forest Fire Danger Index (FFDI; McArthur 1967), and the Energy Release Component (ERC; Bradshaw et al. (1984)). There are two problems with these indices. First, they all incorporate air temperature but not surface net radiation. This means they implicitly model atmospheric evaporative demand as a function of air temperature (PET $= f(T_a)$), rather than net radiation (PET $= f(R_n)$), which is the true control on PET. Apart from performing poorly empirically (Maes et al., 2019), prior literature has shown that temperature-based estimates of PET exaggerate future drying even more than VPD or Penman-based

estimates (Sheffield et al., 2012). Second, wildfire indices are constructed somewhat arbitrarily, with no unique physical mapping to measurable state variables or fluxes (e.g., fuel moisture content or evapotranspiration). While an index may correlate empirically with a measurable quantity in the present climate, there is no guarantee that it will continue to do so as the climate changes. In addition, without a clear, physical link to a measurable variable, it is unclear how to quantify an index's error, which renders it unfalsifiable. These problems also apply to other indices related to drought and aridity (McColl et al., 2022).

Finally, we emphasize that our projections based on soil moisture do show increases in burned forest area by a factor of two to three in the western U.S. by the end of the century. We argue, however, that current projections relying on VPD severely overstate future wildfire risks, a significant problem that results in real costs. Long-term adaptation to climate change, by both public institutions and private actors, depends on accurate and credible risk assessments. As of March 2026, California's largest private insurers have pulled back from the state (Hemmati et al., 2025). While many factors likely contributed to this decision, heightened perceptions of future wildfire risk have been part of the broader context in which these choices were made.

Conflict of Interest

The authors declare no conflicts of interest relevant to this study.

Availability Statement

The Western U.S. MTBS-Interagency (WUMI) wildfire dataset (Juang & Williams, 2024) is available at DRYAD (https://doi.org/10.5061/dryad.sf7m0cg72). The ERA5 (Hersbach et al. (2023); https://cds.climate.copernicus.eu/datasets/reanalysis-era5-single-levels-monthly-means) and the ERA5-Land (Muñoz-Sabater (2019); https://cds.climate.copernicus.eu/datasets/reanalysis-era5-land-monthly-means) reanalysis data are available through the Climate Data Store (CDS; https://cds.climate.copernicus.eu/) provided by the Copernicus Climate Change Service (C3S). The CMIP6 output is available through the Earth System Grid Federation (ESGF; https://esgf-node.llnl.gov/search/cmip6/). The MERRA-2 reanalysis data (Global Modeling and Assimilation Office (GMAO) & Pawson, 2015a, 2015b) are available through the NASA Goddard Earth Sciences Data and Information Services Center (GES DISC; https://gmao.gsfc.nasa.gov/gmao-products/merra-2/), provided by the Global Modeling and Assimilation Office (GMAO).

Acknowledgments

Thanks to David Battisti, Stephen Burges, Park Williams and Jack Scheff for helpful feedback and discussions on this topic. K. A.M. acknowledges funding from NSF Grant AGS-2129576, an NSF CAREER award (AGS-2441565), and a Sloan Research Fellowship (FG-2023-19963). We acknowledge the World Climate Research Programme, which, through its Working Group on Coupled Modelling, coordinated and promoted CMIP6. We thank the climate modeling groups for producing and making available their model output, the Earth System Grid Federation (ESGF) for archiving the data and providing access, and the multiple funding agencies who support CMIP6 and ESGF. We acknowledge the Copernicus Climate Change Service (C3S) for providing access to ERA5 reanalysis data and CMIP6 climate projections via the Climate Data Store (CDS). We also acknowledge the NASA Global Modeling and Assimilation Office (GMAO) for providing access to MERRA-2 reanalysis data through the Goddard Earth Sciences Data and Information Services Center (GES DISC).

References

Abatzoglou, J. T., Battisti, D. S., Williams, A. P., Hansen, W. D., Harvey, B. J., & Kolden, C. A. (2021). Projected increases in western US forest fire despite growing fuel constraints. *Communications Earth & Environment*, *2*(1), 227. https://doi.org/10.1038/s43247-021-00299-0

Abatzoglou, J. T., & Kolden, C. A. (2013). Relationships between climate and macroscale area burned in the western United States. *International Journal of Wildland Fire*, *22*(7), 1003–1020. https://doi.org/10.1071/WF13019

Abatzoglou, J. T., & Williams, A. P. (2016). Impact of anthropogenic climate change on wildfire across western US forests. *Proceedings of the National Academy of Sciences of the United States of America*, *113*(42), 11770–11775. https://doi.org/10.1073/pnas.1607171113

Abatzoglou, J. T., Williams, A. P., Boschetti, L., Zubkova, M., & Kolden, C. A. (2018). Global patterns of interannual climate–fire relationships. *Global Change Biology*, *24*(11), 5164–5175. https://doi.org/10.1111/gcb.14405

Abolafia-Rosenzweig, R., He, C., & Chen, F. (2022). Winter and spring climate explains a large portion of interannual variability and trend in western US summer fire burned area. *Environmental Research Letters*, *17*(5), 054030. https://doi.org/10.1088/1748-9326/ac6886

Aguilera, R., Corringham, T., Gershunov, A., & Benmarhnia, T. (2021). Wildfire smoke impacts respiratory health more than fine particles from other sources: Observational evidence from southern California. *Nature Communications*, *12*(1), 1493. https://doi.org/10.1038/s41467-021-21708-0

Akaike, H. (1998). Information theory and an extension of the maximum likelihood principle. In E. Parzen, K. Tanabe, & G. Kitagawa (Eds.), *Selected papers of Hirotugu Akaike* (pp. 199–213). Springer. https://doi.org/10.1007/978-1-4612-1694-015

Alduchov, O. A., & Eskridge, R. E. (1996). Improved Magnus form approximation of saturation vapor pressure. *Journal of Applied Meteorology and Climatology*, *35*(4), 601–609. https://doi.org/10.1175/1520-0450(1996)035<0601:IMFAOS>2.0.CO;2

Allen, R. G., Pereira, L. S., Raes, D., & Smith, M. (1998). Crop evapotranspiration-guidelines for computing crop water requirements-FAO irrigation and drainage paper 56. *Fao, Rome*, *300*(9), D05109. https://doi.org/10.1038/s41612-020-00137-8

Anderson, D. B. (1936). Relative humidity or vapor pressure deficit. *Ecology*, *17*(2), 277–282. https://doi.org/10.2307/1931468

Balsamo, G., Beljaars, A., Scipal, K., Viterbo, P., Hurk, B. V. D., Hirschi, M., & Betts, A. K. (2009). A revised hydrology for the ECMWF model: Verification from field site to terrestrial water storage and impact in the integrated forecast system. *Journal of Hydrometeorology*, *10*(3), 623–643. https://doi.org/10.1175/2008JHM1068.1

Bayham, J., Yoder, J. K., Champ, P. A., & Calkin, D. E. (2022). The economics of wildfire in the United States. *Annual Review of Resource Economics*, *14*(1), 379–401. https://doi.org/10.1146/annurev-resource-111920-014804

Becker, T., & Stevens, B. (2014). Climate and climate sensitivity to changing CO_2 on an idealized land planet. *Journal of Advances in Modeling Earth Systems*, *6*(4), 1205–1223. https://doi.org/10.1002/2014MS000369

Berg, A., & McColl, K. A. (2021). No projected global drylands expansion under greenhouse warming. *Nature Climate Change*, *11*(4), 331–337. https://doi.org/10.1038/s41558-021-01007-8

Betts, A. K. (2000). Idealized model for equilibrium boundary layer over land. *Journal of Hydrometeorology*, *1*(6), 507–523. https://doi.org/10.1175/1525-7541(2000)001<0507:IMFEBL>2.0.CO;2

Bhattarai, H., Val Martin, M., Sitch, S., Yung, D. H. Y., & Tai, A. P. K. (2025). Global wildfire patterns and drivers under climate change. *Biogeosciences*, *22*(23), 7591–7610. https://doi.org/10.5194/bg-22-7591-2025

Bouchet, R. (1963). Evapotranspiration reelle, evapotranspiration potentielle, et production agricole. *Annales Agronomiques*, *14*, 743–824.

Bradshaw, L. S., Deeming, J. E., Burgan, R. E., & Cohen, J. D. (1984). The 1978 national fire-danger rating system: Technical documentation. In *General technical report INT-169* (Vol. 44, p. 169). US Department of Agriculture, Forest Service, Intermountain Forest and Range Experiment Station. https://doi.org/10.2737/int-gtr-169

Brey, S. J., Barnes, E. A., Pierce, J. R., Swann, A. L., & Fischer, E. V. (2021). Past variance and future projections of the environmental conditions driving western US summertime wildfire burn area. *Earth's Future*, *9*(2), e2020EF001645. https://doi.org/10.1029/2020EF001645

Brown, E. K., Wang, J., & Feng, Y. (2021). US wildfire potential: A historical view and future projection using high-resolution climate data. *Environmental Research Letters*, *16*(3), 034060. https://doi.org/10.1088/1748-9326/aba868

Brutsaert, W., & Stricker, H. (1979). An advection-aridity approach to estimate actual regional evapotranspiration. *Water Resources Research*, *15*(2), 443–450. https://doi.org/10.1029/WR015i002p00443

Burnham, K. P., Anderson, D. R., & Anderson, D. R. (2010). *Model selection and multimodel inference: A practical information-theoretic approach* (2. ed.). Springer.

Clarke, H., Nolan, R. H., De Dios, V. R., Bradstock, R., Griebel, A., Khanal, S., & Boer, M. M. (2022). Forest fire threatens global carbon sinks and population centres under rising atmospheric water demand. *Nature Communications*, *13*(1), 7161. https://doi.org/10.1038/s41467-022-34966-3

Connolly, R., Marlier, M. E., Garcia-Gonzales, D. A., Wilkins, J., Su, J., Bekker, C., et al. (2024). Mortality attributable to $PM_{2.5}$ from wildland fires in California from 2008 to 2018. *Science Advances*, *10*(23), eadl1252. https://doi.org/10.1126/sciadv.adl1252

Copernicus Climate Change Service (C3S). (2021). CMIP6 climate projections. https://doi.org/10.24381/cds.c866074c

Copernicus Climate Change Service (C3S). (2023). ERA5 monthly averaged data on pressure levels from 1940 to present. https://doi.org/10.24381/cds.6860a573

Dahl, K. A., Abatzoglou, J. T., Phillips, C. A., Ortiz-Partida, J. P., Licker, R., Merner, L. D., & Ekwurzel, B. (2023). Quantifying the contribution of major carbon producers to increases in vapor pressure deficit and burned area in western US and southwestern Canadian forests. *Environmental Research Letters*, *18*(6), 064011. https://doi.org/10.1088/1748-9326/acbce8

Delworth, T., & Manabe, S. (1989). The influence of soil wetness on near-surface atmospheric variability. *Journal of Climate*, *2*(12), 1447–1462. https://doi.org/10.1175/1520-0442(1989)002<1447:TIOSWO>2.0.CO;2

Dennison, P. E., Brewer, S. C., Arnold, J. D., & Moritz, M. A. (2014). Large wildfire trends in the western United States, 1984–2011. *Geophysical Research Letters*, *41*(8), 2928–2933. https://doi.org/10.1002/2014GL059576

Dorigo, W., Himmelbauer, I., Aberer, D., Schremmer, L., Petrakovic, I., Zappa, L., et al. (2021). The International Soil Moisture Network: Serving Earth system science for over a decade. *Hydrology and Earth System Sciences*, *25*(11), 5749–5804. https://doi.org/10.5194/hess-25-5749-2021

Eidenshink, J., Schwind, B., Brewer, K., Zhu, Z.-L., Quayle, B., & Howard, S. (2007). A project for monitoring trends in burn severity. *Fire Ecology*, *3*(1), 3–21. https://doi.org/10.4996/fireecology.0301003

Entekhabi, D., Njoku, E. G., O'Neill, P. E., Kellogg, K. H., Crow, W. T., Edelstein, W. N., et al. (2010). The Soil Moisture Active Passive (SMAP) Mission. *Proceedings of the IEEE*, *98*(5), 704–716. https://doi.org/10.1109/JPROC.2010.2043918

Eyring, V., Bony, S., Meehl, G. A., Senior, C. A., Stevens, B., Stouffer, R. J., & Taylor, K. E. (2016). Overview of the Coupled Model Intercomparison Project phase 6 (CMIP6) experimental design and organization. *Geoscientific Model Development*, *9*(5), 1937–1958. https://doi.org/10.5194/gmd-9-1937-2016

Famiglietti, J. S., Ryu, D., Berg, A. A., Rodell, M., & Jackson, T. J. (2008). Field observations of soil moisture variability across scales. *Water Resources Research*, *44*(1), 2006WR005804. https://doi.org/10.1029/2006WR005804

Feldman, A. F., Short Gianotti, D. J., Dong, J., Akbar, R., Crow, W. T., McColl, K. A., et al. (2023). Remotely sensed soil moisture can capture dynamics relevant to plant water uptake. *Water Resources Research*, *59*(2), e2022WR033814. https://doi.org/10.1029/2022WR033814

Feng, X., Mickley, L. J., Kaplan, J. O., Kelp, M., Li, Y., & Liu, T. (2025). Large role of anthropogenic climate change in driving smoke concentrations across the western United States from 1992 to 2020. *Proceedings of the National Academy of Sciences of the United States of America*, *122*(49), e2421903122. https://doi.org/10.1073/pnas.2421903122

Finney, M. A. (1998). *Farsite: Fire area simulator—Model development and evaluation (Research Paper No. RMRS-RP-4). Ogden, UT*. U.S. Department of Agriculture, Forest Service, Rocky Mountain Research Station. https://doi.org/10.2737/RMRS-RP-4

Flannigan, M. D., Logan, K. A., Amiro, B. D., Skinner, W. R., & Stocks, B. J. (2005). Future area burned in Canada. *Climate Change*, *72*(1), 1–16. https://doi.org/10.1007/s10584-005-5935-y

Gallagher, T., & McColl, K. A. (2025). Climate-scale variability in soil moisture explained by a simple theory. *Geophysical Research Letters*, *52*(8), e2025GL115044. https://doi.org/10.1029/2025GL115044

Gelaro, R., McCarty, W., Suárez, M. J., Todling, R., Molod, A., Takacs, L., et al. (2017). The Modern-Era Retrospective analysis for Research and Applications, version 2 (MERRA-2). *Journal of Climate*, *30*(14), 5419–5454. https://doi.org/10.1175/JCLI-D-16-0758.1

Global Modeling and Assimilation Office (GMAO), & Pawson, S. (2015a). MERRA-2 tavgm_2d_lnd_nx: 2d, monthly mean, time-averaged, single-level assimilation land surface diagnostics (version 5.12.4). *NASA Goddard Earth Sciences Data and Information Services Center (GES DISC)*. https://doi.org/10.5067/8S35XF81C28F

Global Modeling and Assimilation Office (GMAO), & Pawson, S. (2015b). MERRA-2 tavgm_2d_slv_nx: 2d, monthly mean, time-averaged, single-level assimilation diagnostics (version 5.12.4). *NASA Goddard Earth Sciences Data and Information Services Center (GES DISC)*. https://doi.org/10.5067/AP1B0BA5PD2K

Greve, P., Roderick, M. L., Ukkola, A. M., & Wada, Y. (2019). The aridity Index under global warming. *Environmental Research Letters*, *14*(12), 124006. https://doi.org/10.1088/1748-9326/ab5046

Gruber, A., Su, C.-H., Zwieback, S., Crow, W., Dorigo, W., & Wagner, W. (2016). Recent advances in (soil moisture) triple collocation analysis. *International Journal of Applied Earth Observation and Geoinformation*, *45*, 200–211. https://doi.org/10.1016/j.jag.2015.09.002

He, Q., Williams, A. P., Johnston, M. R., Juang, C. S., & Wang, B. (2025). Influence of time-averaging of climate data on estimates of atmospheric vapor pressure deficit and inferred relationships with wildfire area in the western United States. *Geophysical Research Letters*, *52*(7), e2024GL113708. https://doi.org/10.1029/2024GL113708

Hemmati, M., Gray, I. P., & Bowen, S. G. (2025). The growing void in the US homeowners insurance market: Who should bear the rising cost of climate change? *npj Climate Action*, *4*(1), 35. https://doi.org/10.1038/s44168-025-00231-8

Hersbach, H., Bell, B., Berrisford, P., Biavati, G., Horányi, A., Muñoz Sabater, J., et al. (2023). ERA5 monthly averaged data on single levels from 1940 to present. *Copernicus Climate Change Service (C3S) Climate Data Store (CDS)*. https://doi.org/10.24381/cds.f17050d7

Hersbach, H., Bell, B., Berrisford, P., Hirahara, S., Horányi, A., Muñoz-Sabater, J., et al. (2020). The ERA5 global reanalysis. *Quarterly Journal of the Royal Meteorological Society*, *146*(730), 1999–2049. https://doi.org/10.1002/qj.3803

Higuera, P. E., & Abatzoglou, J. T. (2021). Record-setting climate enabled the extraordinary 2020 fire season in the western United States. *Global Change Biology*, *27*(1), 1–2. https://doi.org/10.1111/gcb.15388

Holden, Z. A., Swanson, A., Luce, C. H., Jolly, W. M., Maneta, M., Oyler, J. W., et al. (2018). Decreasing fire season precipitation increased recent western US forest wildfire activity. *Proceedings of the National Academy of Sciences of the United States of America*, *115*(36), E8349–E8357. https://doi.org/10.1073/pnas.1802316115

Holden, Z. A., Swanson, A. K., Sadegh, M., Luce, C. H., Noonan-Wright, E., & Parsons, R. A. (2025). Soil moisture is a stronger predictor of Forest fire spread potential than weather in the U.S. Northern rocky Mountains. *Geophysical Research Letters*, *52*(16), e2025GL116248. https://doi.org/10.1073/10.1029/2025GL116248

Hurteau, M. D., Liang, S., Westerling, A. L., & Wiedinmyer, C. (2019). Vegetation-fire feedback reduces projected area burned under climate change. *Scientific Reports*, *9*(1), 2838. https://doi.org/10.1038/s41598-019-39284-1

Hurvich, C. M., & Tsai, C. (1989). Regression and time series model selection in small samples. *Biometrika*, *76*(2), 297–307. https://doi.org/10.1093/biomet/76.2.297

IPCC. (2023). Sections. In Core Writing Team, H. Lee, & J. Romero (Eds.), *Climate change 2023: Synthesis report. Contribution of working groups I, II and III to the Sixth Assessment Report of the Intergovernmental Panel on Climate Change* (pp. 35–115). IPCC. https://doi.org/10.59327/IPCC/AR6-9789291691647

Jackson, T. J., & Schmugge, T. J. (1991). Vegetation effects on the microwave emission of soils. *Remote Sensing of Environment*, *36*(3), 203–212. https://doi.org/10.1016/0034-4257(91)90057-D

Juang, C., & Williams, A. (2024). Western US MTBS-interagency (WUMI) wildfire dataset. *Dryad*. https://doi.org/10.5061/dryad.sf7m0cg72

Juang, C., Williams, A., Abatzoglou, J., Balch, J., Hurteau, M., & Moritz, M. (2022). Rapid growth of large forest fires drives the exponential response of annual forest-fire area to aridity in the western United States. *Geophysical Research Letters*, *49*(5), e2021GL097131. https://doi.org/10.1029/2021GL097131

Juckes, M., Taylor, K. E., Durack, P. J., Lawrence, B., Mizielinski, M. S., Pamment, A., et al. (2020). The CMIP6 data request (dreq, version 01.00. 31). *Geoscientific Model Development*, *13*(1), 201–224. https://doi.org/10.5194/gmd-13-201-2020

Keetch, J. J., & Byram, G. M. (1968). A drought index for forest fire control. In *Research Paper SE-38* (Vol. 35, p. 38). US Department of Agriculture, Forest Service, Southeastern Forest Experiment Station.

Kim, Y., Garcia, M., & Johnson, M. S. (2023). Land-atmosphere coupling constrains increases to potential evaporation in a warming climate: Implications at local and global scales. *Earth's Future*, *11*(2), e2022EF002886. https://doi.org/10.1029/2022EF002886

Koster, R. D., Guo, Z., Yang, R., Dirmeyer, P. A., Mitchell, K., & Puma, M. J. (2009). On the nature of soil moisture in land surface models. *Journal of Climate*, *22*(16), 4322–4335. https://doi.org/10.1175/2009JCLI2832.1

Koster, R. D., Suarez, M. J., Ducharne, A., Stieglitz, M., & Kumar, P. (2000). A catchment-based approach to modeling land surface processes in a general circulation model: 1. Model structure. *Journal of Geophysical Research*, *105*(D20), 24809–24822. https://doi.org/10.1029/2000JD900327

Krakauer, N., Cook, B., & Puma, M. (2010). Contribution of soil moisture feedback to hydroclimatic variability. *Hydrology and Earth System Sciences*, *14*(3), 505–520. https://doi.org/10.5194/hess-14-505-2010

Krawchuk, M. A., & Moritz, M. A. (2011). Constraints on global fire activity vary across a resource gradient. *Ecology*, *92*(1), 121–132. https://doi.org/10.1890/09-1843.1

Krueger, E. S., Levi, M. R., Achieng, K. O., Bolten, J. D., Carlson, J. D., Coops, N. C., et al. (2023). Using soil moisture information to better understand and predict wildfire danger: A review of recent developments and outstanding questions. *International Journal of Wildland Fire*, *32*(2), 111–132. https://doi.org/10.1071/wf22056

Laguë, M., Quetin, G., & Boos, W. (2023). Reduced terrestrial evaporation increases atmospheric water vapor by generating cloud feedbacks. *Environmental Research Letters*, *18*(7), 074021. https://doi.org/10.1088/1748-9326/acdbe1

Li, Y., Mickley, L. J., Liu, P., & Kaplan, J. O. (2020). Trends and spatial shifts in lightning fires and smoke concentrations in response to 21st century climate over the national forests and parks of the western United States. *Atmospheric Chemistry and Physics*, *20*(14), 8827–8838. https://doi.org/10.5194/acp-20-8827-2020

Linn, R., Reisner, J., Colman, J. J., & Winterkamp, J. (2002). Studying wildfire behavior using FIRETEC. *International Journal of Wildland Fire*, *11*(4), 233–246. https://doi.org/10.1071/WF02007

Littell, J. S., & Gwozdz, R. B. (2011). Climatic water balance and regional fire years in the Pacific Northwest, USA: Linking regional climate and fire at landscape scales. In D. McKenzie, C. Miller, & D. A. Falk (Eds.), *The landscape ecology of fire* (pp. 117–139). Springer Netherlands. https://doi.org/10.1007/978-94-007-0301-8_5

Littell, J. S., McKenzie, D., Peterson, D. L., & Westerling, A. L. (2009). Climate and wildfire area burned in western US ecoprovinces, 1916–2003. *Ecological Applications*, *19*(4), 1003–1021. https://doi.org/10.1890/07-1183.1

Littell, J. S., McKenzie, D., Wan, H. Y., & Cushman, S. A. (2018). Climate change and future wildfire in the western United States: An ecological approach to nonstationarity. *Earth's Future*, *6*(8), 1097–1111. https://doi.org/10.1029/2018EF000878

Liu, J. C., Wilson, A., Mickley, L. J., Dominici, F., Ebisu, K., Wang, Y., et al. (2017). Wildfire-specific fine particulate matter and risk of hospital admissions in urban and rural counties. *Epidemiology*, *28*(1), 77–85. https://doi.org/10.1097/EDE.0000000000000556

Lu, Y., & Wei, C. (2021). Evaluation of microwave soil moisture data for monitoring live fuel moisture content (LFMC) over the coterminous United States. *Science of the Total Environment*, *771*, 145410. https://doi.org/10.1016/j.scitotenv.2021.145410

Maes, W. H., Gentine, P., Verhoest, N. E. C., & Miralles, D. G. (2019). Potential evaporation at eddy-covariance sites across the globe. *Hydrology and Earth System Sciences*, *23*(2), 925–948. https://doi.org/10.5194/hess-23-925-2019

Marlon, J. R., Bartlein, P. J., Gavin, D. G., Long, C. J., Anderson, R. S., Briles, C. E., et al. (2012). Long-term perspective on wildfires in the western USA. *Proceedings of the National Academy of Sciences of the United States of America*, *109*(9), E535–E543. https://doi.org/10.1073/pnas.1112839109

Matthews, T. K., Wilby, R. L., & Murphy, C. (2017). Communicating the deadly consequences of global warming for human heat stress. *Proceedings of the National Academy of Sciences of the United States of America*, *114*(15), 3861–3866. https://doi.org/10.1073/pnas.1617526114

McArthur, A. G. (1967). *Fire behaviour in eucalypt forests*. Forestry and Timber Bureau.

McColl, K. A., & Rigden, A. J. (2020). Emergent simplicity of continental evapotranspiration. *Geophysical Research Letters*, *47*(6), e2020GL087101. https://doi.org/10.1029/2020GL087101

McColl, K. A., Roderick, M. L., Berg, A., & Scheff, J. (2022). The terrestrial water cycle in a warming world. *Nature Climate Change*, *12*(7), 604–606. https://doi.org/10.1038/s41558-022-01412-7

McColl, K. A., & Tang, L. I. (2024). An analytic theory of near-surface relative humidity over land. *Journal of Climate*, *37*(4), 1213–1230. https://doi.org/10.1175/JCLI-D-23-0342.1

McKenzie, D., & Littell, J. S. (2017). Climate change and the eco-hydrology of fire: Will area burned increase in a warming western USA? *Ecological Applications*, *27*(1), 26–36. https://doi.org/10.1002/eap.1420

Milly, P. C., & Dunne, K. A. (2016). Potential evapotranspiration and continental drying. *Nature Climate Change*, *6*(10), 946–949. https://doi.org/10.1038/nclimate3046

Morton, F. (1969). Potential evaporation as a manifestation of regional evaporation. *Water Resources Research*, *5*(6), 1244–1255. https://doi.org/10.1029/WR005i006p01244

Mueller, S. E., Thode, A. E., Margolis, E. Q., Yocom, L. L., Young, J. D., & Iniguez, J. M. (2020). Climate relationships with increasing wildfire in the southwestern US from 1984 to 2015. *Forest Ecology and Management*, *460*, 117861. https://doi.org/10.1016/j.foreco.2019.117861

Muñoz-Sabater, J. (2019). ERA5-land monthly averaged data from 1950 to present. *Copernicus Climate Change Service (C3S) Climate Data Store (CDS)*. https://doi.org/10.24381/cds.68d2bb30

Muñoz-Sabater, J., Dutra, E., Agustí-Panareda, A., Albergel, C., Arduini, G., Balsamo, G., et al. (2021). ERA5-Land: A state-of-the-art global reanalysis dataset for land applications. *Earth System Science Data*, *13*(9), 4349–4383. https://doi.org/10.5194/essd-13-4349-2021

NOAA National Centers for Environmental Information. (2025). Climate change: Global temperature. Retrieved from https://www.climate.gov/news-features/understanding-climate/climate-change-global-temperature

O'Neill, B. C., Tebaldi, C., Van Vuuren, D. P., Eyring, V., Friedlingstein, P., Hurtt, G., et al. (2016). The Scenario Model Intercomparison Project (ScenarioMIP) for CMIP6. *Geoscientific Model Development*, *9*(9), 3461–3482. https://doi.org/10.5194/gmd-9-3461-2016

Palmer, W. C. (1965). Meteorological drought. *Weather Bureau Research Paper*, *45*, 1–58.

Parks, S. A., & Abatzoglou, J. T. (2020). Warmer and drier fire seasons contribute to increases in area burned at high severity in western US forests from 1985 to 2017. *Geophysical Research Letters*, *47*(22), e2020GL089858. https://doi.org/10.1029/2020GL089858

Parks, S. A., Miller, C., Parisien, M.-A., Holsinger, L. M., Dobrowski, S. Z., & Abatzoglou, J. (2015). Wildland fire deficit and surplus in the western United States, 1984–2012. *Ecosphere*, *6*(12), 1–13. https://doi.org/10.1890/ES15-00294.1

Pechony, O., & Shindell, D. (2009). Fire parameterization on a global scale. *Journal of Geophysical Research*, *114*(D16). https://doi.org/10.1029/2009JD011927

Pellizzaro, G., Cesaraccio, C., Duce, P., Ventura, A., & Zara, P. (2007). Relationships between seasonal patterns of live fuel moisture and meteorological drought indices for mediterranean shrubland species. *International Journal of Wildland Fire*, *16*(2), 232–241. https://doi.org/10.1071/WF06081

Pfeiffer, M., Spessa, A., & Kaplan, J. O. (2013). A model for global biomass burning in preindustrial time: LPJ-LMfire (v1.0). *Geoscientific Model Development*, *6*(3), 643–685. https://doi.org/10.5194/gmd-6-643-2013

Price, C., & Rind, D. (1994). The impact of a 2× CO_2 climate on lightning-caused fires. *Journal of Climate*, *7*(10), 1484–1494. https://doi.org/10.1175/1520-0442(1994)007<1484:TIOACC>2.0.CO;2

Qi, Y., Dennison, P. E., Spencer, J., & Riaño, D. (2012). Monitoring live fuel moisture using soil moisture and remote sensing proxies. *Fire Ecology*, *8*(3), 71–87. https://doi.org/10.4996/fireecology.0803071

Qiu, M., Li, J., Gould, C. F., Jing, R., Kelp, M., Childs, M. L., et al. (2025). Wildfire smoke exposure and mortality burden in the US under climate change. *Nature*, *647*, 1–3. https://doi.org/10.1038/s41586-025-09611-w

Ray, D., Nepstad, D., & Moutinho, P. (2005). Micrometeorological and canopy controls of fire susceptibility in a forested Amazon landscape. *Ecological Applications*, *15*(5), 1664–1678. https://doi.org/10.1890/05-0404

Reichle, R. H., Draper, C. S., Liu, Q., Girotto, M., Mahanama, S. P. P., Koster, R. D., & Lannoy, G. J. M. D. (2017). Assessment of MERRA-2 land surface hydrology estimates. *Journal of Climate*, *30*(8), 2937–2960. https://doi.org/10.1175/JCLI-D-16-0720.1

Roderick, M. L., Greve, P., & Farquhar, G. D. (2015). On the assessment of aridity with changes in atmospheric CO_2. *Water Resources Research*, *51*(7), 5450–5463. https://doi.org/10.1002/2015WR017031

Ruefenacht, B., Finco, M., Nelson, M., Czaplewski, R., Helmer, E., Blackard, J., et al. (2008). Conterminous US and Alaska forest type mapping using forest inventory and analysis data. *Photogrammetric Engineering & Remote Sensing*, *74*(11), 1379–1388. https://doi.org/10.14358/PERS.74.11.1379

Seager, R., Hooks, A., Williams, A. P., Cook, B., Nakamura, J., & Henderson, N. (2015). Climatology, variability, and trends in the US vapor pressure deficit, an important fire-related meteorological quantity. *Journal of Applied Meteorology and Climatology*, *54*(6), 1121–1141. https://doi.org/10.1175/JAMC-D-14-0321.1

Sedano, F., & Randerson, J. (2014). Multi-scale influence of vapor pressure deficit on fire ignition and spread in boreal forest ecosystems. *Biogeosciences*, *11*(14), 3739–3755. https://doi.org/10.5194/bg-11-3739-2014

Sharma, S., Carlson, J., Krueger, E. S., Engle, D. M., Twidwell, D., Fuhlendorf, S. D., et al. (2020). Soil moisture as an indicator of growing-season herbaceous fuel moisture and curing rate in grasslands. *International Journal of Wildland Fire*, *30*(1), 57–69. https://doi.org/10.1071/WF19193

Sheffield, J., Wood, E. F., & Roderick, M. L. (2012). Little change in global drought over the past 60 years. *Nature*, *491*(7424), 435–438. https://doi.org/10.1038/nature11575

Sherwood, S., & Fu, Q. (2014). A drier future? *Science*, *343*(6172), 737–739. https://doi.org/10.1126/science.1247620

Silvestrini, R. A., Soares-Filho, B. S., Nepstad, D., Coe, M., Rodrigues, H., & Assunção, R. (2011). Simulating fire regimes in the Amazon in response to climate change and deforestation. *Ecological Applications*, *21*(5), 1573–1590. https://doi.org/10.1890/10-0827.1

Sørensen, Ø., Frigessi, A., & Thoresen, M. (2015). Measurement error in lasso: Impact and likelihood bias correction. *Statistica Sinica*, *25*, 809–829. https://doi.org/10.5705/ss.2013.180

Spracklen, D. V., Mickley, L. J., Logan, J. A., Hudman, R. C., Yevich, R., Flannigan, M. D., & Westerling, A. L. (2009). Impacts of climate change from 2000 to 2050 on wildfire activity and carbonaceous aerosol concentrations in the western United States. *Journal of Geophysical Research*, *114*(D20). https://doi.org/10.1029/2008JD010966

Tang, L. I., & McColl, K. A. (2025). Radiative-convective equilibrium over an idealized land surface with fixed soil moisture. *Journal of Climate*, *38*(22), 6639–6659. https://doi.org/10.1175/JCLI-D-24-0438.1

Thonicke, K., Spessa, A., Prentice, I., Harrison, S. P., Dong, L., & Carmona-Moreno, C. (2010). The influence of vegetation, fire spread and fire behaviour on biomass burning and trace gas emissions: Results from a process-based model. *Biogeosciences*, *7*(6), 1991–2011. https://doi.org/10.5194/bg-7-1991-2010

Thonicke, K., Venevsky, S., Sitch, S., & Cramer, W. (2001). The role of fire disturbance for global vegetation dynamics: Coupling fire into a dynamic global vegetation model. *Global Ecology and Biogeography*, *10*(6), 661–677. https://doi.org/10.1046/j.1466-822X.2001.00175.x

Tibshirani, R. (1996). Regression shrinkage and selection via the lasso. *Journal of the Royal Statistical Society Series B: Statistical Methodology*, *58*(1), 267–288. https://doi.org/10.1111/j.2517-6161.1996.tb02080.x

Turco, M., Abatzoglou, J. T., Herrera, S., Zhuang, Y., Jerez, S., Lucas, D. D., et al. (2023). Anthropogenic climate change impacts exacerbate summer forest fires in California. *Proceedings of the National Academy of Sciences of the United States of America*, *120*(25), e2213815120. https://doi.org/10.1073/pnas.2213815120

U.S. Environmental Protection Agency. (2024). Ecoregions of North America. Retrieved from https://www.epa.gov/eco-research/ecoregions-north-america

Vargas Zeppetello, L. R., McColl, K. A., Bernau, J. A., Bowen, B. B., Tang, L. I., Holbrook, N. M., et al. (2023). Apparent surface conductance sensitivity to vapour pressure deficit in the absence of plants. *Nature Water*, *1*(11), 941–951. https://doi.org/10.1038/s44221-023-00147-9

Wagner, C. V. (1987). Development and structure of the Canadian forest fire weather index system. In *Canadian forestry service forestry technical report*.

Westerling, A. L. (2016). Increasing western US forest wildfire activity: Sensitivity to changes in the timing of spring. *Philosophical Transactions of the Royal Society B*, *371*(1696), 20150178. https://doi.org/10.1098/rstb.2015.0178

Westerling, A. L., Bryant, B. P., Preisler, H. K., Holmes, T. P., Hidalgo, H. G., Das, T., & Shrestha, S. R. (2011). Climate change and growth scenarios for California wildfire. *Climate Change*, *109*(S1), 445–463. https://doi.org/10.1007/s10584-011-0329-9

Westerling, A. L., Turner, M. G., Smithwick, E. A., Romme, W. H., & Ryan, M. G. (2011). Continued warming could transform greater Yellowstone fire regimes by mid-21st century. *Proceedings of the National Academy of Sciences of the United States of America*, *108*(32), 13165–13170. https://doi.org/10.1073/pnas.1110199108

Western, A. W., Grayson, R. B., & Blöschl, G. (2002). Scaling of soil moisture: A hydrologic perspective. *Annual Review of Earth and Planetary Sciences*, *30*(1), 149–180. https://doi.org/10.1146/annurev.earth.30.091201.140434

Williams, A. P., & Abatzoglou, J. T. (2016). Recent advances and remaining uncertainties in resolving past and future climate effects on global fire activity. *Current Climate Change Reports*, *2*, 1–14. https://doi.org/10.1007/s40641-016-0031-0

Williams, A. P., Abatzoglou, J. T., Gershunov, A., Guzman-Morales, J., Bishop, D. A., Balch, J. K., & Lettenmaier, D. P. (2019). Observed impacts of anthropogenic climate change on wildfire in California. *Earth's Future*, *7*(8), 892–910. https://doi.org/10.1029/2019EF001210

Williams, A. P., Allen, C. D., Macalady, A. K., Griffin, D., Woodhouse, C. A., Meko, D. M., et al. (2013). Temperature as a potent driver of regional forest drought stress and tree mortality. *Nature Climate Change*, *3*(3), 292–297. https://doi.org/10.1038/nclimate1693

Williams, A. P., Seager, R., Macalady, A. K., Berkelhammer, M., Crimmins, M. A., Swetnam, T. W., et al. (2014). Correlations between components of the water balance and burned area reveal new insights for predicting forest fire area in the southwest United States. *International Journal of Wildland Fire*, *24*(1), 14–26. https://doi.org/10.1071/WF14023

Yang, Y., Roderick, M. L., Zhang, S., McVicar, T. R., & Donohue, R. J. (2019). Hydrologic implications of vegetation response to elevated CO_2 in climate projections. *Nature Climate Change*, *9*(1), 44–48. https://doi.org/10.1038/s41558-018-0361-0

Yue, X., Mickley, L. J., Logan, J. A., & Kaplan, J. O. (2013). Ensemble projections of wildfire activity and carbonaceous aerosol concentrations over the western United States in the mid-21st century. *Atmospheric Environment*, *77*, 767–780. https://doi.org/10.1016/j.atmosenv.2013.06.003

Zhou, S., Williams, A. P., Berg, A. M., Cook, B. I., Zhang, Y., Hagemann, S., et al. (2019). Land–atmosphere feedbacks exacerbate concurrent soil drought and atmospheric aridity. *Proceedings of the National Academy of Sciences*, *116*(38), 18848–18853. https://doi.org/10.1073/pnas.1904955116

Zhou, S., & Yu, B. (2024). Physical basis of the potential evapotranspiration and its estimation over land. *Journal of Hydrology*, *641*, 131825. https://doi.org/10.1016/j.jhydrol.2024.131825

Zhou, S., & Yu, B. (2025a). Neglecting land–atmosphere feedbacks overestimates climate-driven increases in evapotranspiration. *Nature Climate Change*, *15*(10), 1–8. https://doi.org/10.1038/s41558-025-02428-5

Zhou, S., & Yu, B. (2025b). Reconciling the discrepancy in projected global dryland expansion in a warming world. *Global Change Biology*, *31*(3), e70102. https://doi.org/10.1111/gcb.70102

Zhuang, Y., Fu, R., Santer, B. D., Dickinson, R. E., & Hall, A. (2021). Quantifying contributions of natural variability and anthropogenic forcings on increased fire weather risk over the western United States. *Proceedings of the National Academy of Sciences of the United States of America*, *118*(45), e2111875118. https://doi.org/10.1073/pnas.2111875118

Large overestimation of projected western U.S. wildfire burned forest area with warming

Yu Cheng[1,2], **Kaighin A. McColl**[2,3], **Loretta J. Mickley**[3], **Xu Feng**[3]

[1]Shanghai Key Laboratory of Ocean-land-atmosphere Boundary Dynamics and Climate Change, Department of Atmospheric and Oceanic Sciences, Fudan University, Shanghai, China
[2]Department of Earth and Planetary Sciences, Harvard University, Cambridge, Massachusetts, USA
[3]School of Engineering and Applied Sciences, Harvard University, Cambridge, Massachusetts, USA

Contents of this file

Corresponding author: Kaighin A. McColl, kmccoll@seas.harvard.edu

Table S1. CMIP6 models used in this study and their approximate atmospheric horizontal resolutions. For each model, we analyzed output from the Historical (1984–2014), SSP1-2.6 (2015–2099), SSP2-4.5 (2015–2099), SSP3-7.0 (2015–2099), and SSP5-8.5 (2015–2099) experiments.

Model name	Horizontal resolution (lon × lat)
ACCESS-CM2	1.875° × 1.25°
CESM2	1.25° × 0.9375°
CMCC-CM2-SR5	1.25° × 0.9375°
CNRM-CM6-1-HR	0.5° × 0.5°
CNRM-ESM2-1	1.4063° × 1.4063°
CanESM5-CanOE	2.8125° × 2.8125°
KACE-1-0-G	1.875° × 1.25°
MIROC-ES2L	2.8125° × 2.8125°
MIROC6	1.4063° × 1.4063°
MPI-ESM1-2-LR	1.875° × 1.875°
MRI-ESM2-0	1.125° × 1.125°
UKESM1-0-LL	1.875° × 1.25°

Table S2. Squared Pearson correlation (R^2) between the logarithm of burned forest area and VPD anomaly, and between the logarithm of burned forest area and soil moisture anomaly. The 95% bootstrap confidence intervals are shown in brackets. For each ecoregion, the percentage of total burned forest area in the western U.S. occurring in that ecoregion is shown. The percentages do not add up to exactly 100% due to rounding.

Region	Percentage of total burned forest area	VPD	Soil moisture
Whole domain	100%	0.73 (0.54, 0.85)	0.74 (0.51, 0.86)
Ecoregion 1	73.2%	0.76 (0.60, 0.86)	0.76 (0.60, 0.85)
Ecoregion 2	4.6%	0.08 (0, 0.35)	0.05 (0, 0.26)
Ecoregion 3	7.9%	0.35 (0.11, 0.58)	0.22 (0.05, 0.43)
Ecoregion 4	12.7%	0.72 (0.54, 0.83)	0.66 (0.39, 0.82)
Ecoregion 5	1.9%	0.40 (0.12, 0.67)	0.27 (0.02, 0.64)

Table S3. Same as Table S2 but for MERRA-2 reanalysis.

Region	Percentage of total burned forest area	VPD	Soil moisture
Whole domain	100%	0.58 (0.33, 0.75)	0.42 (0.14, 0.66)
Ecoregion 1	73.2%	0.64 (0.40, 0.80)	0.44 (0.20, 0.65)
Ecoregion 2	4.6%	0.11 (0.01, 0.30)	0.06 (0.00, 0.21)
Ecoregion 3	7.9%	0.27 (0.04, 0.52)	0.16 (0.00, 0.42)
Ecoregion 4	12.7%	0.59 (0.31, 0.77)	0.55 (0.28, 0.73)
Ecoregion 5	1.9%	0.41 (0.17, 0.64)	0.36 (0.11, 0.62)

Table S4. Same as Table S2 but for ERA5-Land reanalysis.

Region	Percentage of total burned forest area	VPD	Soil moisture
Whole domain	100%	0.76 (0.59, 0.86)	0.70 (0.45, 0.83)
Ecoregion 1	73.2%	0.79 (0.64, 0.88)	0.74 (0.57, 0.83)
Ecoregion 2	4.6%	0.37 (0.04, 0.69)	0.40 (0.13, 0.68)
Ecoregion 3	7.9%	0.46 (0.16, 0.69)	0.34 (0.11, 0.57)
Ecoregion 4	12.7%	0.69 (0.51, 0.81)	0.56 (0.27, 0.75)
Ecoregion 5	1.9%	0.60 (0.24, 0.82)	0.51 (0.15, 0.80)

Table S5. Model selection rates for the two univariate models (VPD or soil moisture) in each region, based on the sample-size corrected Akaike Information Criterion (AIC_c) and using the ERA5 reanalysis. The AIC_c was estimated for each model in each region. The model with the lower AIC_c is considered the better model. To account for sampling uncertainty in model selection, we used bootstrapping with 10,000 replicates to repeat the process by sampling with replacement from the observations, and report the fraction of replicates in which each model was selected as the better model (see Burnham et al. (2010), Section 4.5.2).

Region	VPD	Soil moisture
Whole domain	44%	56%
Ecoregion 1	46%	54%
Ecoregion 2	76%	24%
Ecoregion 3	98%	2%
Ecoregion 4	79%	21%
Ecoregion 5	92%	8%

Table S6. Same as Table S5, but using MERRA-2.

Region	VPD	Soil moisture
Whole domain	99%	1%
Ecoregion 1	100%	0%
Ecoregion 2	82%	18%
Ecoregion 3	95%	5%
Ecoregion 4	73%	27%
Ecoregion 5	79%	21%

Table S7. Same as Table S5, but using ERA5-Land.

Region	VPD	Soil moisture
Whole domain	83%	17%
Ecoregion 1	88%	12%
Ecoregion 2	44%	56%
Ecoregion 3	95%	5%
Ecoregion 4	99%	1%
Ecoregion 5	88%	12%

Table S8. Model selection rates for univariate and multivariate models, based on the sample-size corrected Akaike Information Criterion (AIC_c) and using the ERA5 reanalysis. All models are evaluated over the whole domain. The model with the lowest AIC_c is considered the best model. To account for sampling uncertainty in model selection, we used bootstrapping with 10,000 replicates to repeat the process by sampling with replacement from the observations, and report the fraction of replicates in which each model was selected as the best model (see Burnham et al. (2010), Section 4.5.2).

Model	Model selection rate
Univariate: Soil moisture	49%
Univariate: VPD	34%
Multivariate: all seven variables	3.5%
Multivariate: excluding air temperature	7%
Multivariate: excluding VPD	5%
Multivariate: excluding air temperature and VPD	1.5%

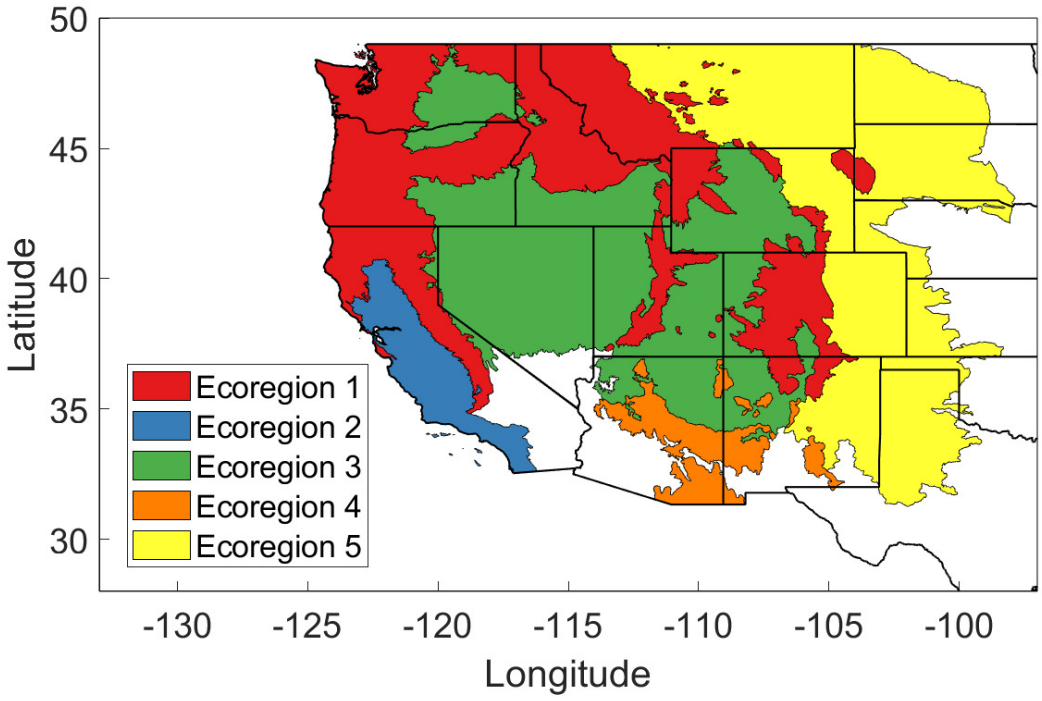

Figure S1. Ecoregions used in this study. The five regions are based on the EPA Level II Ecoregion dataset (U.S. Environmental Protection Agency, 2024). The ecoregions are (1) Northwestern Forested Mountains, (2) Mediterranean California (11.1), (3) Cold Deserts (10.1), (4) Southwestern Forested Mountains, and (5) Central Prairies. Three of these ecoregions are aggregates of smaller ecoregions: Ecoregion 1 consists of the Western cordillera (6.2) and Marine west coast forests (7.1); Ecoregion 4 consists of the Upper Gila mountains (13.1) and the Western Sierra Madre piedmont (12.1); and Ecoregion 5 consists of the West-central semi-arid prairies (9.3) and the South-central semi-arid prairies (9.4). Numbers in the parentheses are the EPA Ecoregion codes.

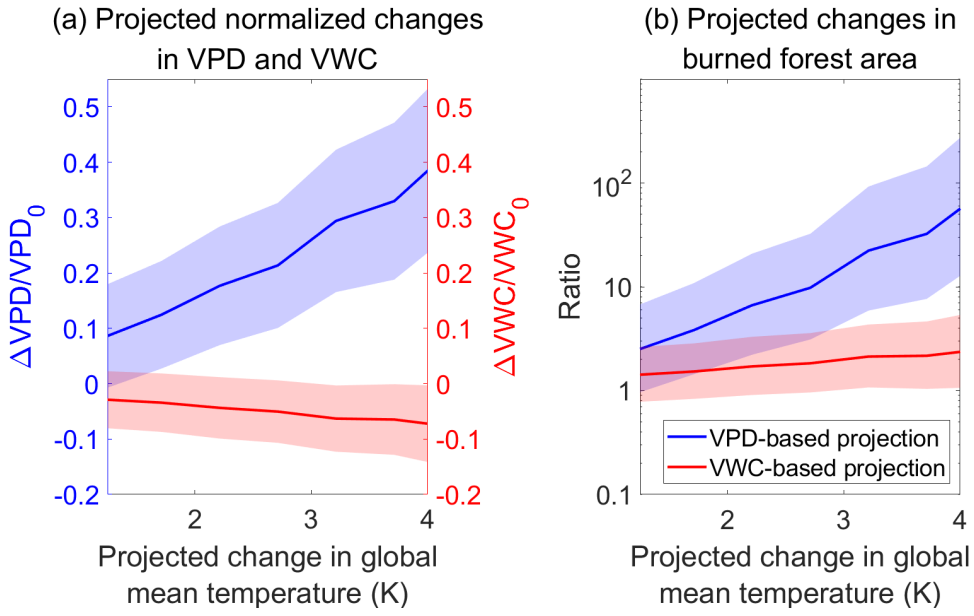

Figure S2. Same as Figure 3 but replacing the absolute values in the y axis with the ratio between absolute values and historical mean.

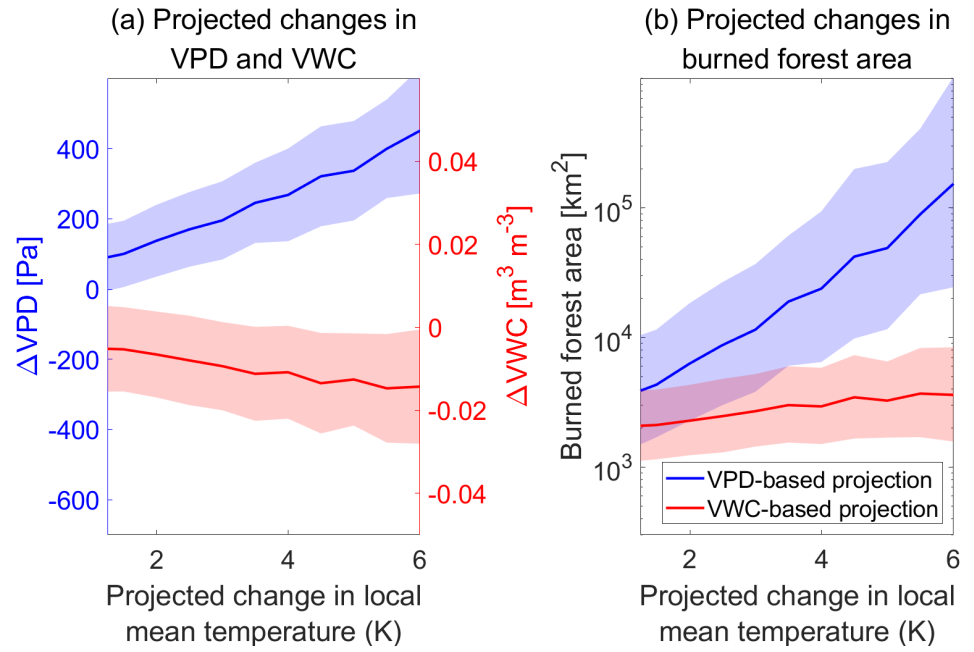

Figure S3. Same as Figure 3 but replacing the x-axis with local temperature change.

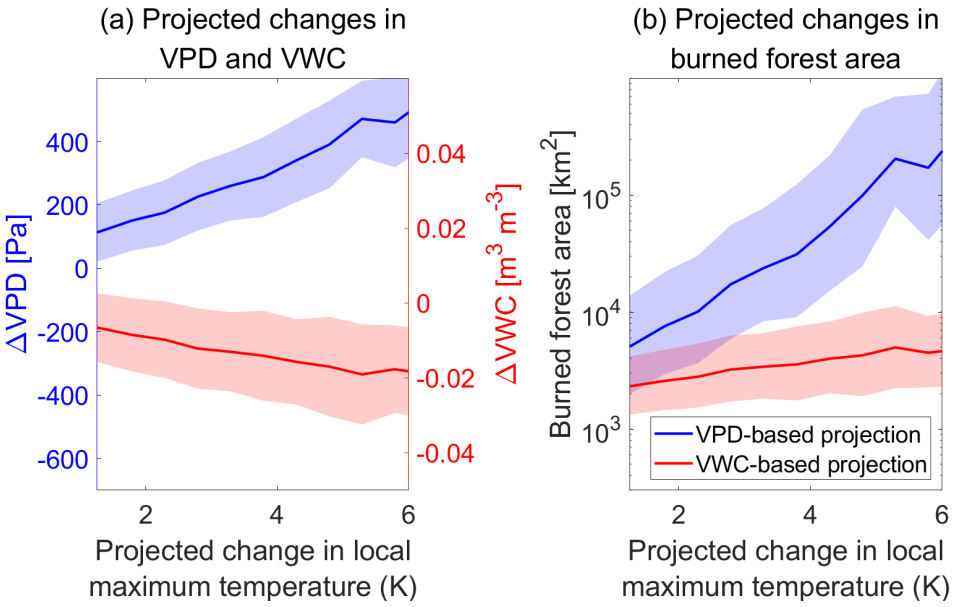

Figure S4. Same as Figure 3 but replacing the x-axis with local maximum temperature change.

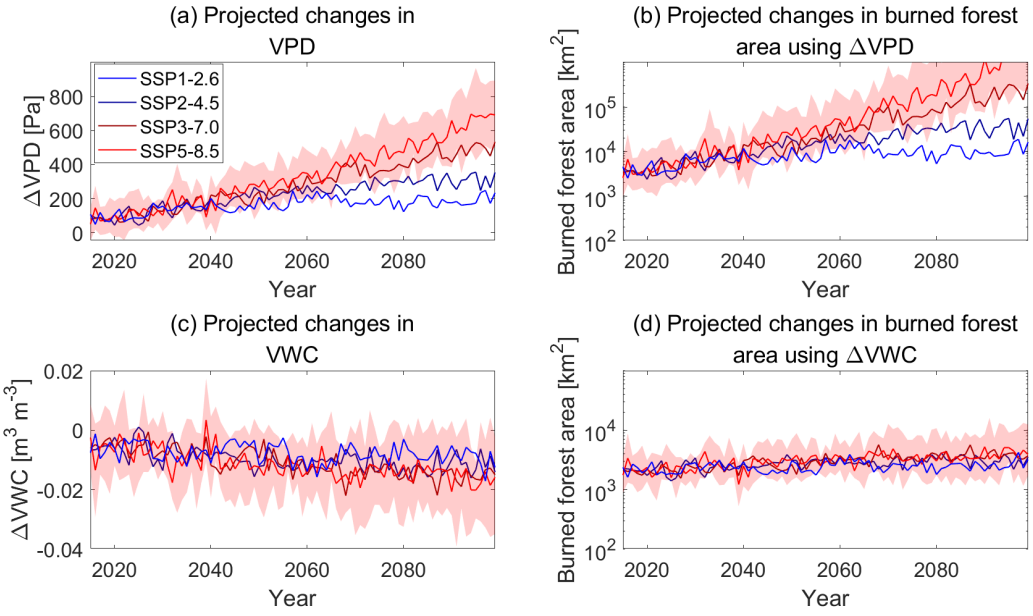

Figure S5. Temporal evolution of (a) ΔVPD and (b) VPD-based projections of burned forest area in the western U.S. during 2015–2099 under SSP1-2.6, SSP2-4.5, SSP3-7.0, and SSP5-8.5. Panels (c) and (d) show the corresponding results using VWC in place of VPD. The shaded region indicates the multi-model mean ± one standard deviation for the scenario SSP5-8.5.

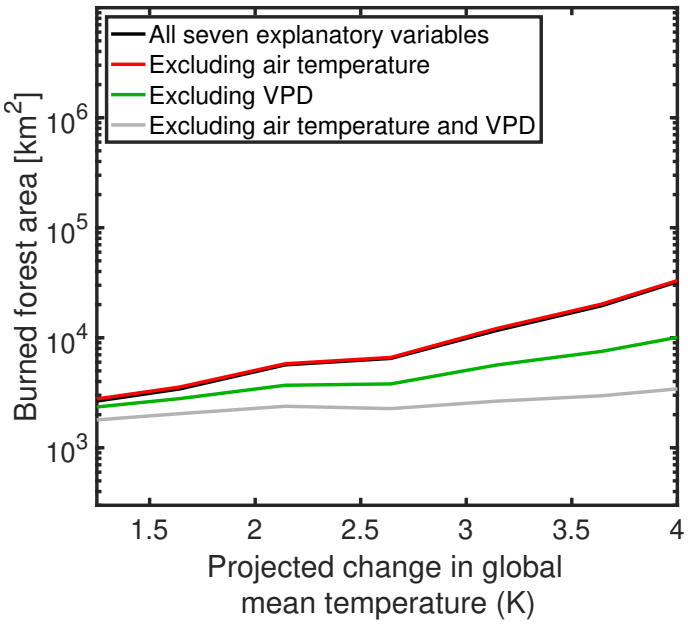

Figure S6. Projections of burned forest area in the western U.S. based on multivariate regressions using seven variables, as described in the main text. Shown are projections obtained using all variables; excluding air temperature; excluding VPD; and excluding both air temperature and VPD.

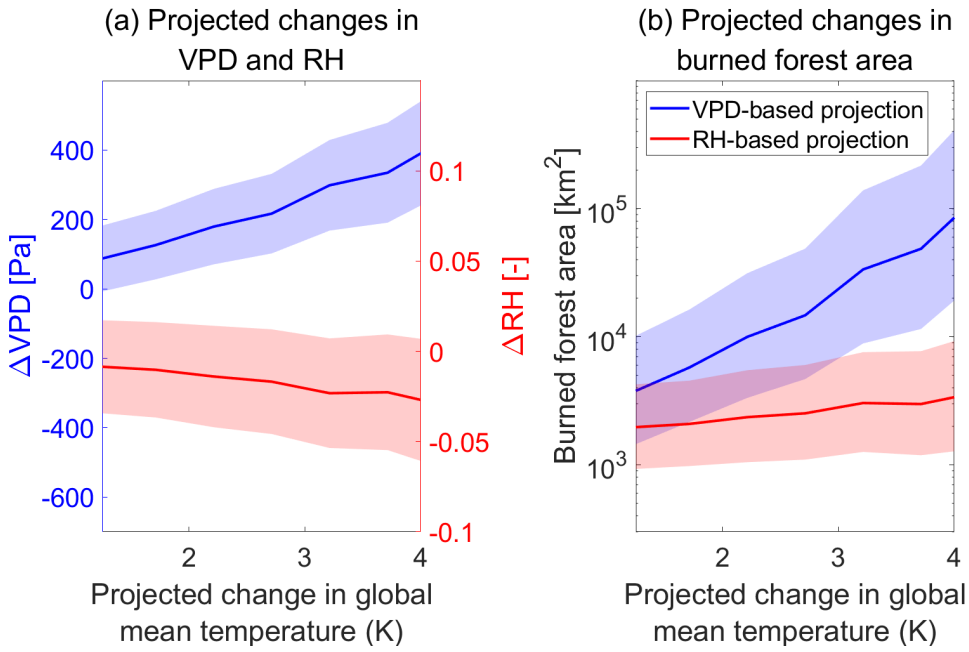

Figure S7. Same as Figure 3 but replacing soil moisture with near-surface relative humidity as the predictor for burned area.

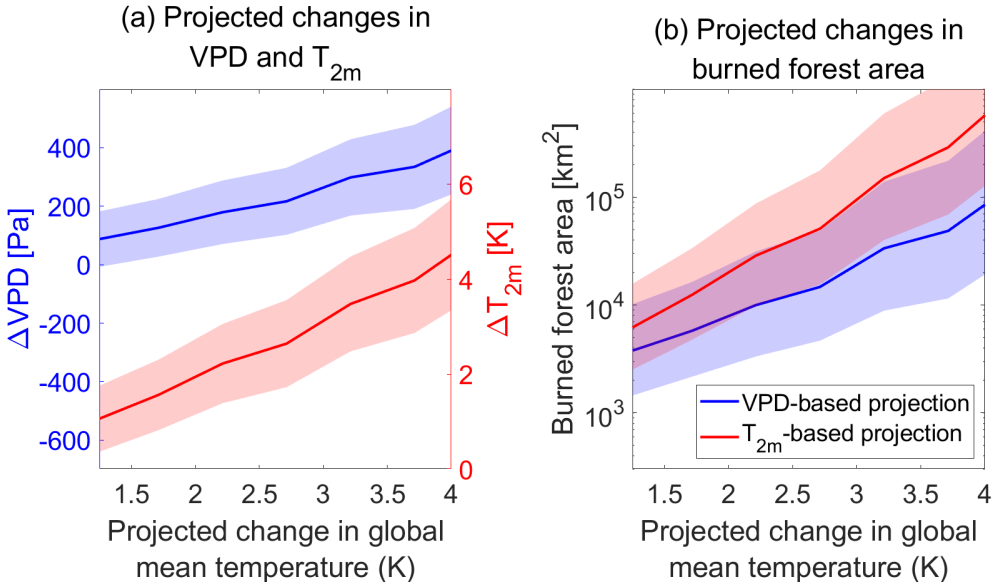

Figure S8. Same as Figure 3 but replacing soil moisture with near-surface air temperature as the predictor for burned area.

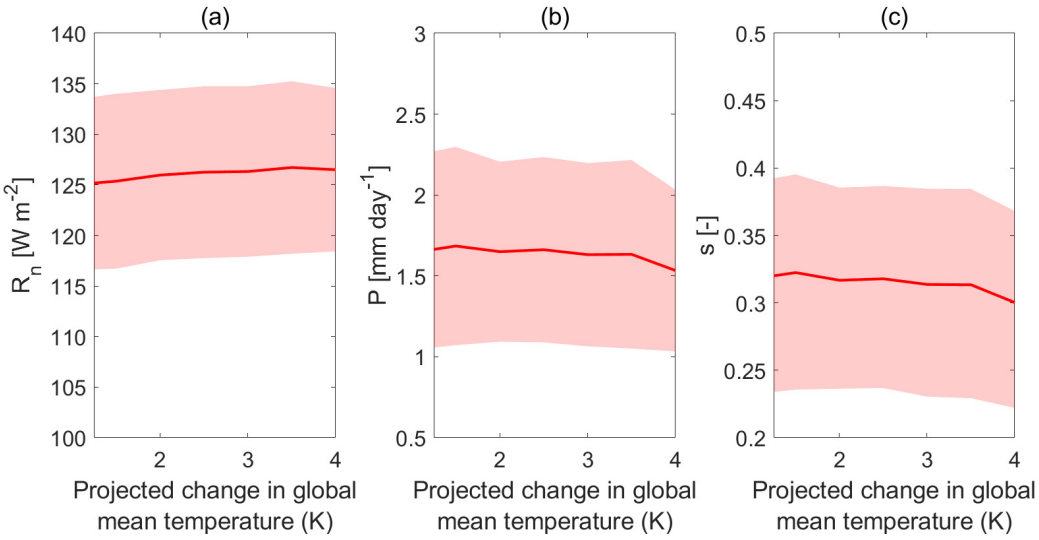

Figure S9. Surface net radiation (R_n), precipitation (P), and the predicted soil saturation (s) plotted against mean global temperature change. R_n and P are from CMIP6 output, and s is calculated using R_n, P and a recent theory for soil moisture (equation 2 of Gallagher and McColl (2025)). The averaging process is the same as that used in Figure 3.

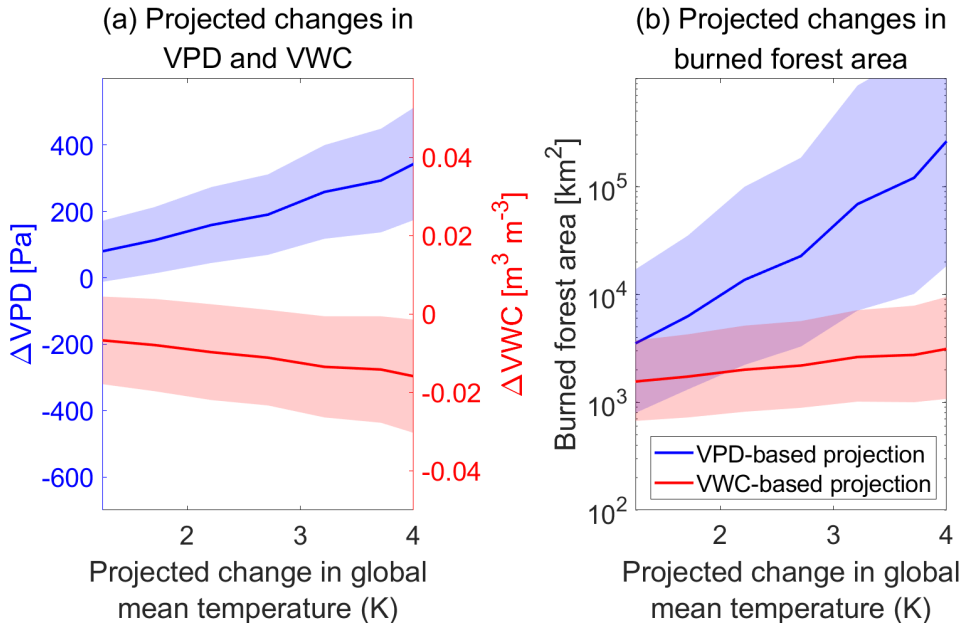

Figure S10. Same as Figure 3 but for Ecoregion 1.

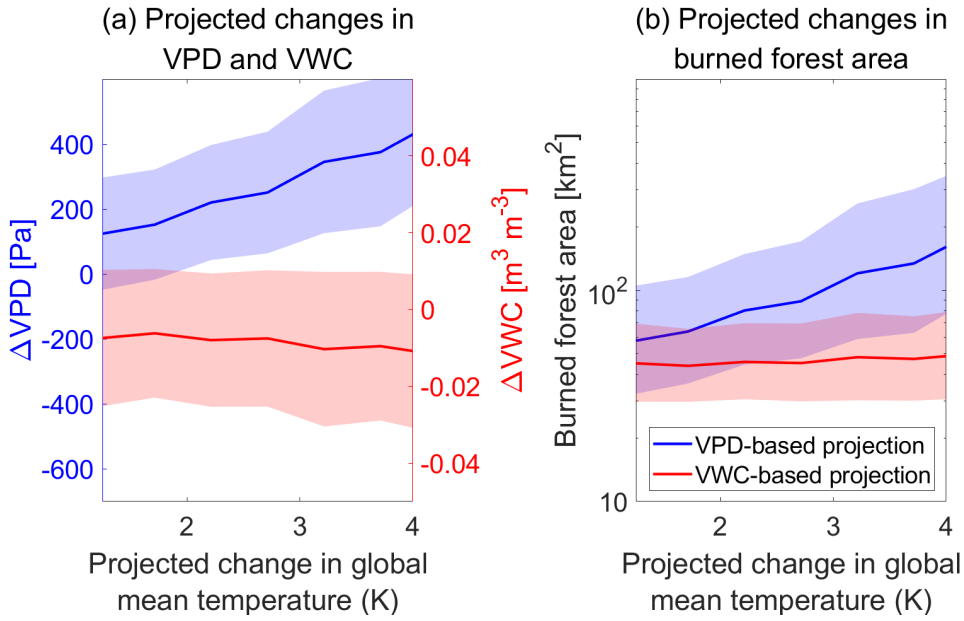

Figure S11. Same as Figure 3 but for Ecoregion 2.

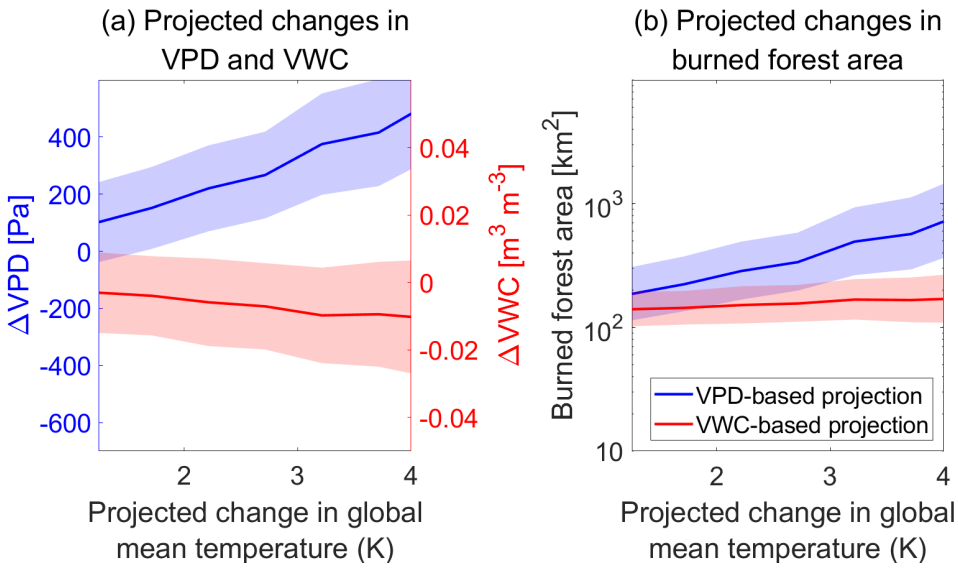

Figure S12. Same as Figure 3 but for Ecoregion 3.

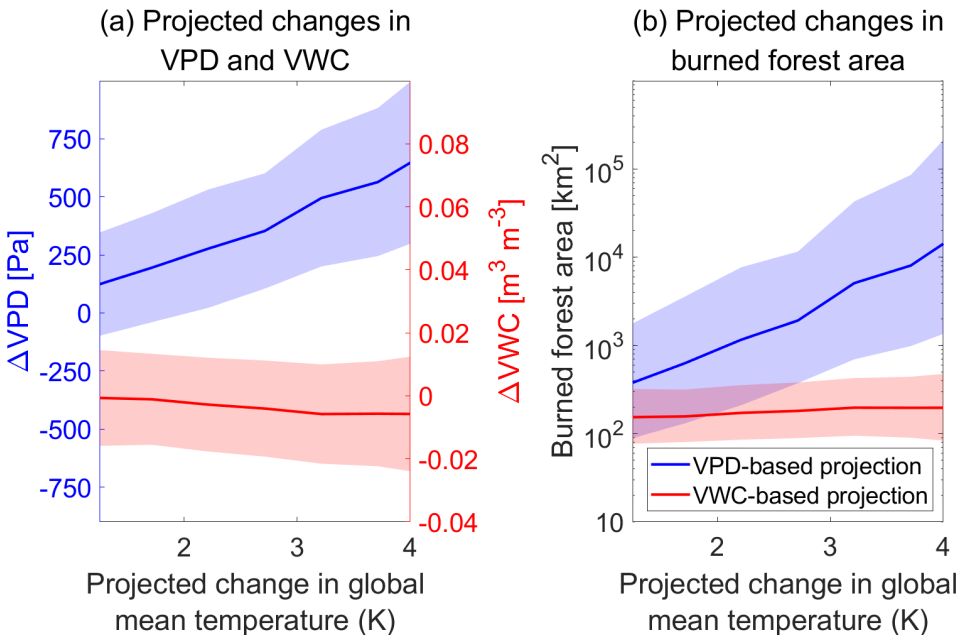

Figure S13. Same as Figure 3 but for Ecoregion 4.

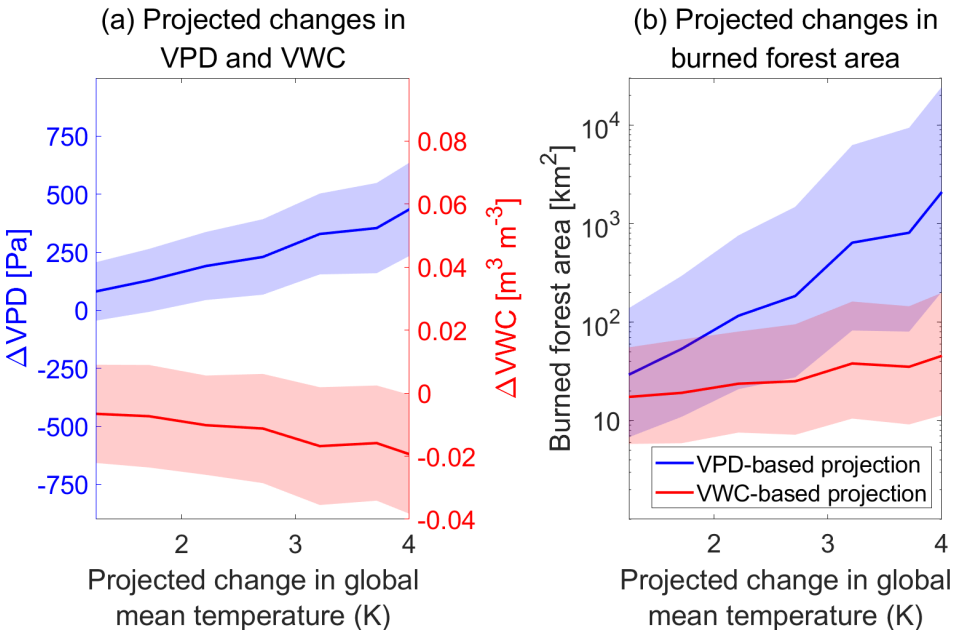

Figure S14. Same as Figure 3 but for Ecoregion 5.

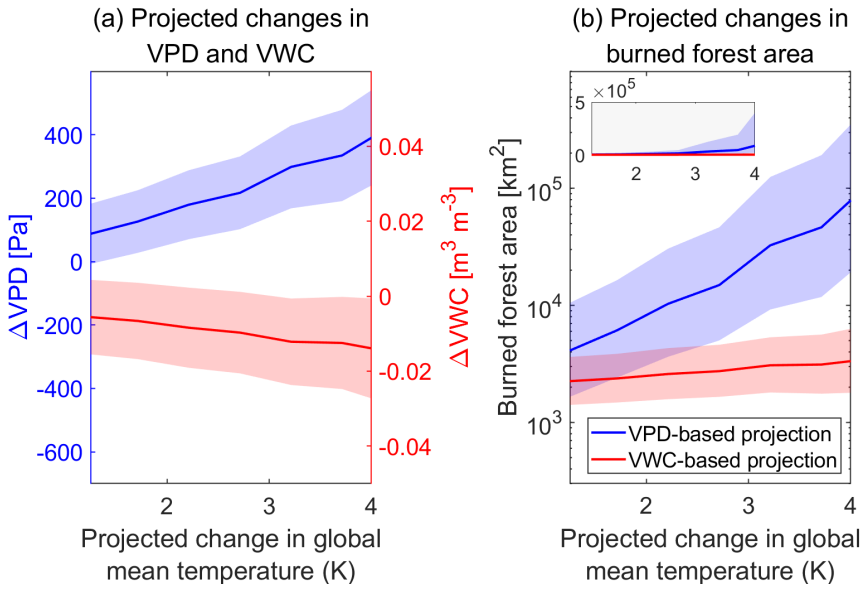

Figure S15. Same as Fig. 3 but using MERRA-2 reanalysis.

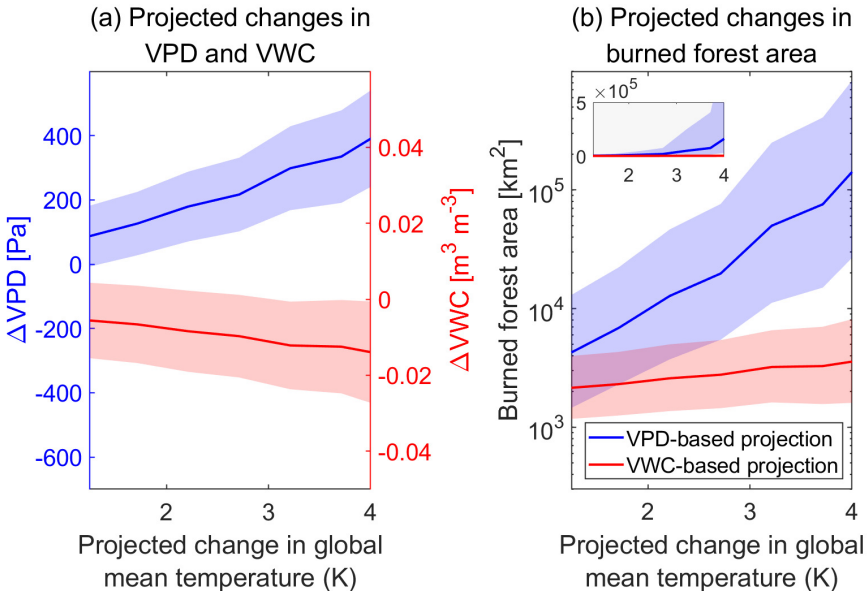

Figure S16. Same as Fig. 3 but using ERA5-Land reanalysis.

References

Burnham, K. P., Anderson, D. R., & Anderson, D. R. (2010). *Model selection and multimodel inference: a practical information-theoretic approach* (2. ed., [4. printing] ed.). New York, NY: Springer.

Gallagher, T., & McColl, K. A. (2025). Climate-scale variability in soil moisture explained by a simple theory. *Geophys. Res. Lett.*, *52*(8), e2025GL115044. https://doi.org/10.1029/2025GL115044.

U.S. Environmental Protection Agency. (2024). *Ecoregions of North America.* https://www.epa.gov/eco-research/ecoregions-north-america.